# Application of machine learning methodology to detect the potential for fluvial hazards to occur along river networks

Marco Gava

A Thesis

in the Department

of

Geography, Planning and Environment

Presented in Partial Fulfillment of the

Requirements for the Degree of Master of Science

(Geography, Urban and Environmental Studies) at Concordia University

Montreal, Quebec, Canada

July 2023

# CONCORDIA UNIVERSITY

## School of Graduate Studies

This is to certify that the thesis prepared

By: Marco Gava

Entitled: Application of machine learning methodology to detect the potential for fluvial hazards to occur along river networks

and submitted in partial fulfillment of the requirements for the degree of

**Master of Science (Geography, Urban and Environmental Studies)**

complies with the regulations of the University and meets the accepted standards with respect

to originality and quality.

Signed by the final Examining Committee:

_____ Examiner and Chair

Dr. Angela Kross

_____ External Examiner

Dr. Peter Ashmore

_____ Supervisor

Dr. Pascale Biron

_____ Supervisor

Dr. Thomas Buffin-Bélanger

Approved by:                                    _____

Dr. Craig Townsend, Chair of Department

_____ 2023                               _____

Date                                            Dr. Pascale Sicotte, Dean of Faculty

# Abstract

## Application of machine learning methodology to detect the potential for fluvial hazards to occur along river networks

## Marco Gava

Fluvial hazards of river mobility and flooding are often problematic for road infrastructure and need to be considered in the planning process. The extent of river and road infrastructure networks and their tendency to be close to each other creates a need to be able to identify the most dangerous areas quickly and cost-effectively. In this study we propose a novel methodology utilizing random forest machine learning methods and hydro geomorphic expertise to provide easily interpretable fine scale fluvial hazard predictions for large fluvial networks. The developed tools provided these predictions at reference points every 100 meters along the fluvial network of three watersheds within the province of Quebec, Canada and used variables focused on river conditions and to proxy hydro geomorphic processes such as sediment transport. Training/validation data was collected in four forms: field data, results from hydraulic and erosion models, government infrastructure databases, and hydro geomorphic evaluations using the 1-m DEM and satellite/historical imagery. First a subset of the reference points was manually classified then divided into training (75%) and validation (25%) datasets. Then the training dataset was used to train supervised random forest models. The validation dataset combined with extensive validation indices indicated the models were capable of accurately predicting the potential for hazards to occur. Metrics are extracted from the model to determine which variables are most important to predict each hazard. Finally, a methodology is proposed for a top-down hazard analysis of extensive fluvial networks to identify the most at-risk infrastructure/communities.

# Acknowledgements

# Contribution of Authors

Chapter 5:

Co-Authors:

Pascale Biron and Thomas Buffin-Bélanger

# Table of Contents

# List of Figures

# List of Tables

# 1) Introduction

Extreme river discharge events can have severe impacts on road infrastructure adjacent to rivers such as bridges, culverts, or roads which can cause subsequent and lasting issues of accessing or evacuating communities impacted by flooding or repairing impacted electrical/communication lines (Brooks & Lawrence, 2000; Pealer, 2012; Anderson et al., 2017; Nasr et al., 2020). According to several climate models, the probability of these large flood events is expected to increase in Quebec (Ouranos, 2015; Ouranos, 2021; IPCC, 2021). Increases in precipitation and large floods are also correlated with increased sediment mobility in rivers (Li & Wei, 2014; Li & Fang, 2016; Wu et al., 2018), which increases the potential of aggradation and degradation in the river causing accumulation of sediments, bank erosion and incision of the riverbeds near river adjacent infrastructure. The federal government of Canada and the provincial government of Quebec have both responded to these changing trends via increased data collection, tool development, flood maps, and incorporation of fluvial hazards into laws (MELCC, 2015; Natural Resources Canada & Public Safety Canada, 2018; CEHQ, 2021; NSERC, 2021; Gouvernement du Québec, 2021; Gouvernement du Québec, 2022).

Sediments carried by rivers have historically been neglected relative to other factors when conceptualizing bridges and culverts in Quebec. However, recent investments have been made to begin implementing sediment dynamics into infrastructure planning via research and tool development (Demers et al., 2014; MELCC, 2015; Scoazec & Buffin-Belanger, 2019). The recent changes relevant for this project are a new regulation requiring river mobility to be assessed prior to the construction of new infrastructure adjacent to a river or dredging activities, and the aim of developing tools to better incorporate fluvial geomorphology into infrastructure and policy planning (MELCC, 2015; Gouvernement du Québec, 2021).

This comes at a time when Quebec has reached its goal of providing high resolution LiDAR (Light Detection And Ranging) elevation data (1 meter resolution) for the southern portion of its territory which is where the majority of the population and infrastructure is located. This new data will allow for high-resolution geographical analyses of hydro-geomorphological processes at large scale. Many open-source Geographical Information System (GIS) tools and models exist to extract geomorphic variables from LiDAR and use them to predict fluvial hazards (Biron et al., 2013; Gartner, 2015; Wheaton et al., 2015; Bangen et al., 2017; Cavalli et al., 2017; Crema & Cavalli, 2018; Scoazec & Buffin-Belanger, 2019; Bernier et al., 2021). However, new methods and techniques need to consider the computational costs of running models on these large datasets (Li et al., 2015; Tavares da Costa, 2019). This project will contribute to the development of fluvial geomorphology tools to better characterize river dynamics, in particular flooding and mobility caused by erosion of the river banks or bed. It will also help accomplish the Quebec government's goal of incorporating river mobility into the assessment of road infrastructure by combining the substantial amounts of available GIS data, knowledge, and tools while minimizing the required computational cost and creating a user-friendly interface.

# 2) Literature Review

This literature review is organized into four sections. The first covers the heterogeneity of river types that exist and how they are defined at various scales. The second section discusses the

factors that impact the frequency and amplitude of fluvial hazards. The third section discusses how geomorphological processes can damage infrastructure crossing or adjacent to a river as well as how anthropogenic modifications to the river can modify the dominant fluvial dynamics. The fourth section consists of a review of some of the available tools used in hydrology and geomorphology and the use of machine learning (ML) models for these applications.

## 2.1) Geomorphic classification and associated hazards

Many types of rivers exist depending on the geomorphological context and the fluvial processes (flooding/erosion) that occur within these river types will differ (Figure 2.1). Rivers are in a dynamic equilibrium between water discharge and sediment discharge, with rivers eroding their bed and banks when the water discharge outweighs the sediment discharge to regain equilibrium and depositing it when the sediment discharge exceeds the water discharge (Leopold, 1962; Fryirs & Brierley, 2013; Sear et al., 2021). This dynamic equilibrium will fluctuate based on the volume of water and sediments in the river but is also influenced by other variables, principally the geomorphic variables of the river such as the slope, width of the channel and confinement but also biotic variables such as vegetation cover extent/type, biotic community, and human interventions (Poff, 2014; Johnson et al., 2020; Sear et al., 2021; Bywater-Reyes et al., 2022; Papangelakis et al., 2022; Ashmore et al., 2023). This combination of the availability of water and sediments, the local geomorphic/biotic variables, and anthropogenic modifications will determine the potential geomorphological processes that may pose a hazard for infrastructure. Using these variables, we can classify rivers at multiple imbricated scales, the combination of which will identify the geomorphological processes active in an area (Brierley & Fryirs, 2004; Beechie et al., 2014; Buffin-Bélanger et al., 2015; Kasprak et al., 2016; Reid & Brierley, 2015).

Many classification systems exist such as the River Styles Framework, Schumm's (1963) classification expanded on by Church (2006), and the Rosgen Classification System (Brierley & Fryirs, 2004; Kasprak et al., 2016; Reid & Brierley, 2015; Horacio et al., 2017; Fryirs & Brierley, 2018; Fryirs et al., 2021). The choice of classification system should be dependent on the goals of the project and data available as they all require various levels of expertise and data (Kasprak et al., 2016; Horacio et al., 2017). It is also important to consider the simplification of river systems inherent in the classification systems and their subjectivity along with the message they will portray to the infrastructure and policy planners who will use the results, as this message can influence their decisions on the course of policy surrounding rivers (Tadaki et al., 2014). Statistical clustering of geomorphic variables has also proven to be a cost-effective method of categorizing rivers at large scale, a method known simply as geomorphic classification of rivers (Kasprak et al., 2016; Horacio et al., 2017). These classifications have been linked to their fluvial dynamics (aggradation, degradation, flooding) which can impact road infrastructure and are also useful for the sustainable management of watersheds. The three most common scales used in these classification systems are the fluvial forms (landscape unit), fluvial style (homogeneous reach), and geomorphic units (small scale), all of which are important to evaluate to properly determine the fluvial processes that will occur locally. Therefore, to properly assess the potential occurrence of fluvial hazards, it is necessary to have variables at several scales in order to take into account the diversity of conditions that will occur at these three scales.

2
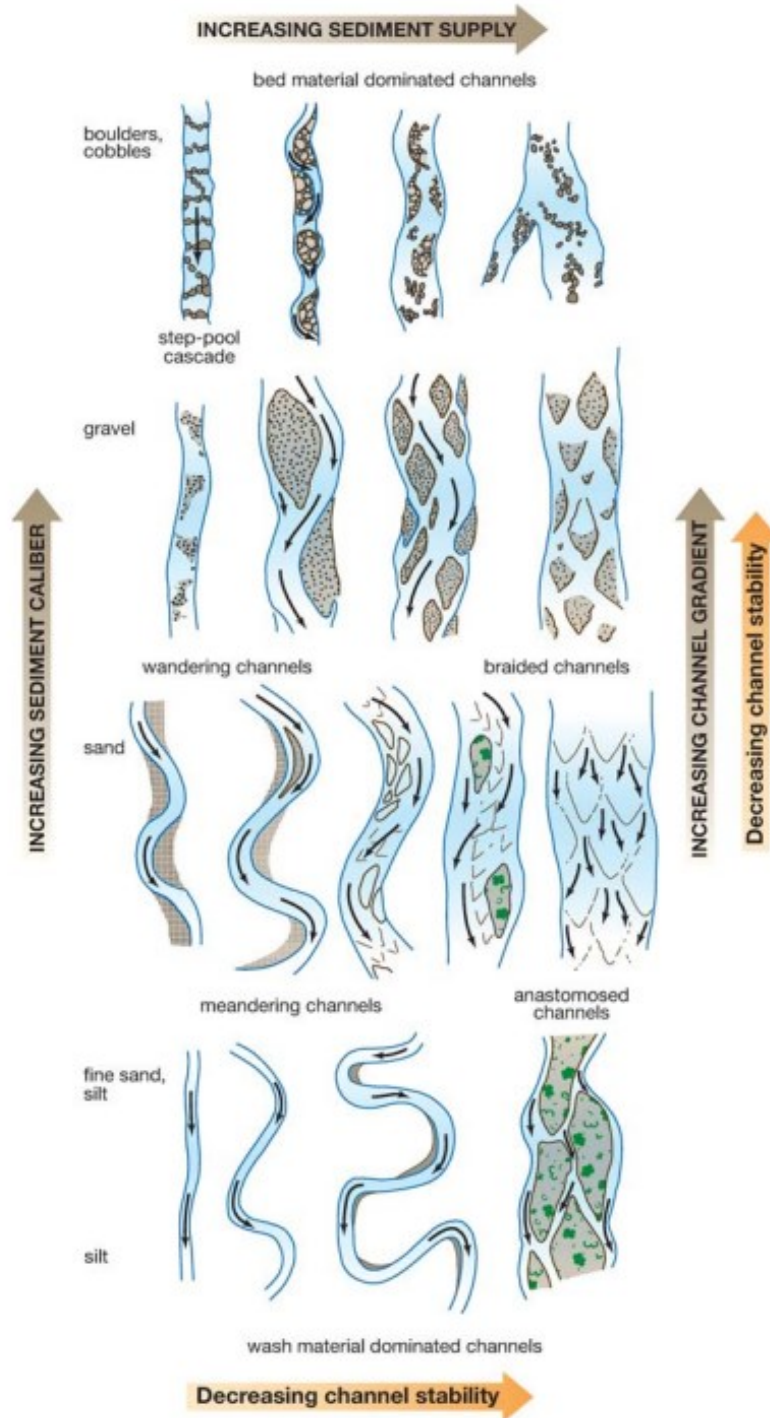
*Figure 2.1: Fluvial styles, how they relate to key variables, and their stability (Church, 2006, after Church 1992).*

### 2.1.1) Valley setting/Fluvial forms

The valley setting operates at the landscape scale and is indicative of a region's availability of erodible sediments and typical geomorphic variables, therefore at the valley setting scale we are examining in which context the river is flowing through rather than examining the river itself (Fryirs & Brierley, 2018). A key variable that exists at this scale,

3

relevant to fluvial hazards, is the way in which the surrounding landscape confines the river, either naturally through non-erodible material or anthropogenically via roads or bank stabilization. This confinement controls the types of hazards that are possible in a river and therefore should be considered when determining the sensitivity of a reach to geomorphic change (Buffin-Bélanger et al., 2015; Reid & Brierley, 2015; Sear et al., 2021; Wheeler et al., 2022). The confinement combined with the type of confining material (bedrock, road, erodible terrace) can be used for the classification of a river's fluvial form which typically includes classes such as canyon (confined and non-erodible), floodplain (partly confined to unconfined with various confining material), delta (unconfined and highly erodible), and alluvial fan (unconfined and highly erodible) (Brierley & Fryirs, 2004; Buffin-Bélanger et al., 2015). These settings will impact the type of fluvial processes that will occur in the river by controlling the level of erosion/flooding possible as well as influencing the quantity and size of sediments flowing from upstream. Canyons which will have low erodible sediment availability in the banks will lead to incision of the canyon bed while floodplains that are unconfined or partly confined with erodible material will have varying hazards such as lateral erosion, flooding, and incision depending on the local confining material and geomorphic variables (Buffin-Bélanger et al., 2015; Reid & Brierley, 2015). Another important fluvial form is alluvial fans which occur when smaller, steeper sloped streams transporting a large caliber of sediment or a large volume of sediments merges with a larger main channel that lacks the energy to move this sudden large increase in sediments and therefore creates a fan-like structure out of these sediments (Mazgareanu et al., 2020). Deltas are also depositional structures which form when rivers deposit their sediments at the edge of a standing body of water such as lakes or oceans. Many varieties of deltas exist depending on the transport capacity of the river versus the power of the tide and waves of the body of water (Seybold et al., 2007). These deltas/alluvial fans can present other risks such as frequent avulsions which can result in rapid and drastic changes in both the volume of water and sediments that may reach culverts or bridges leading to blockages of and damages to the structure or/and flooding of the local area (Buffin-Bélanger et al., 2015; Mazgareanu et al., 2020).

**2.1.2) River planform/fluvial style**

River planforms/fluvial styles are defined at the homogeneous reach scale and are a function of the region's valley setting/fluvial form and of the river channel's geomorphic variables. Homogeneous reaches are defined according to a hydrogeomorphic perspective (Montgomery and Buffington, 1997) and represent channel lengths that contain similar geomorphic variables (confinement, slope, sinuosity, grain size). They are therefore not constant in length. For example, Choné and Biron (2016) had homogeneous reaches ranging between 560 m and 7.8 km in the Yamaska Sud-Est River (Quebec, Canada) whereas Biron et al. (2014) report average homogenous reaches ranging between 1 and 7.3 km in three rivers in Quebec where the freedom space was mapped. In Quebec, the CRHQ (Cadre de Référence Hydrologique du Québec) is a database that contain spatial units called UEA (Unités Écologiques Aquatiques) which are based on similar concepts to hydrogeomorphological homogeneous reaches, and which can therefore be used in automated GIS tools.

There exist many classifications of channels at this scale with the six major ones being linear, stable meandering, dynamic meandering, wandering, anastomosed, and braided channels (Buffin-Bélanger et al., 2015; Fryirs & Brierley, 2018). These can be distinguished using geomorphic variables such as the slope, presence of bars, the sinuosity of the channels and the

4

number of channels but are also reliant on the availability of erodible sediments and their size provided by the local fluvial form (Buffin-Bélanger et al., 2015). Identifying the fluvial style is important to determine the river's ability to shape the landscape it is flowing through with the various fluvial styles having differing hazards that can impact road infrastructure as well as differing levels of sensitivity to those hazards (Buffin-Bélanger et al., 2015; Reid & Brierley, 2015; Wheeler et al., 2022). Fluvial styles will often consist of more than one geomorphic unit or a sequence of geomorphic units such as the pool/riffle complexes typical of meandering rivers (Buffin-Bélanger et al., 2015). It is therefore important to consider variables at the homogenous reach scale to further our understanding of which fluvial dynamics will dominate. Variables at this scale such as the sinuosity are important to consider in fluvial dynamic assessments as highly sinuous (meandering) rivers tend to have higher rates of lateral migration relative to linear rivers which are more likely to be incising.

**2.1.3) Geomorphic unit**

Geomorphic unit is the finest scale that is potentially detectable using LiDAR data. These units describe morphologies in both the river channel and the surrounding floodplain. Geomorphic units are a result of the geomorphic variables, the vegetative cover, land use, as well as larger scale processes such as erodible/transportable sediment availability (Bangen et al., 2017; Belletti et al., 2017). Some examples of in-channel geomorphic units are pools, rifles, central and point bars, and secondary channels, while some examples for the floodplain geomorphic units are alluvial terrasse, unvegetated banks, and floodplains (Bangen et al., 2017; Belletti et al., 2017; Williams et al., 2020; *Geomorphic Unit Quick Reference Guide*, 2022). These units are created and modified by the local fluvial processes altering the banks and bed of the river such as pools forming due to natural or anthropogenically caused scouring or riffles forming due to a local deposition of sediments (Buffin-Bélanger et al., 2015; Williams et al., 2020; Fryirs & Brierley, 2022; *Geomorphic Unit Quick Reference Guide*, 2022). This makes geomorphic units useful in determining which areas within a homogenous reach are prone to erosion or deposition as these are the processes that created and maintain the geomorphic units (Bangen et al., 2017; Fryirs & Brierley, 2018; Fryirs & Brierley, 2022). To properly identify the geomorphic units, it is important to consider the larger-scale variable as the geomorphic units are influenced by the fluvial form and style with the dominating fluvial process, upstream conditions and confining materials impacting the types of geomorphic units that are present in a homogenous reach. Some examples are waterfalls typically occurring in geologically confined areas and levees being typically found in actively meandering rivers (Fryirs & Brierley, 2022). The location of in-channel sediment accumulations (bars) can also be indicative of the fluvial style as actively meandering rivers will have alluvial point bars in the curves while braided rivers will have central bars, whilst other fluvial styles will have both or alternate bars (Buffin-Bélanger et al., 2015; Fryirs & Brierley, 2022). The size of these bars and whether they are growing or shrinking is also an indication of the upstream availability of sediments, with growing bars indicating that sediments are widely available due to processes such as landslides and shrinking bars associated with reduced flux of sediments from upstream (Buffin-Bélanger et al., 2015). Geomorphic units are the most precise indication of the dominating fluvial processes, however their presence is strongly influenced by larger-scale variables that need to be taken into account to correctly distinguish geomorphological units and determine the extent to which the fluvial processes that created them are still active.

5

## 2.2) Variables influencing fluvial processes

### 2.2.1) Geomorphic sensitivity and availability of sediments

The geomorphic sensitivity of the landscape as well as the quantity and size of sediments attaining the reach can be indicative of the future trajectory of a river reach (Reid & Brierley, 2015; Lisenby et al., 2020). Geomorphic sensitivity refers to the landscape's ability to resist fluvial erosion and is the result of the local geomorphic variables of both the landscape the river is flowing through as well as the river (Reid & Brierley, 2015; Lisenby et al., 2020). Many of these local variables have become measurable at large scale in GIS, such as the slope and width of the river (Biron et al., 2013; Beechie et al., 2014; Gartner et al., 2016), whereas proxies need to be used for others such as quantity and size of sediments attaining the reach and river discharge (Biron et al., 2013; Sear et al., 2021).

A river's capacity to transport sediments and erode the landscape comes from a combination of its liquid discharge and local geomorphic variables (Leopold, 1962). A key variable to quantify the amount of energy a river has to potentially mobilize sediments and predict this transport capacity is total (TSP, in W/m) and unit (USP, in W/m$^2$) stream power (Sear et al., 2021), which was originally derived by Bagnold (1966), and is proportional to discharge (Q) and channel slope (S):

$$TSP = \rho \, g \, Q \, S \tag{2.1}$$

$$USP = TSP / W \tag{2.2}$$

where $\rho$ is water density, g is acceleration due to gravity and W is channel width. Unit stream power is useful for determining a reach's geomorphic sensitivity as it can be used to predict areas where erosion and deposition are likely to occur (Yochum et al., 2017; Sear et al., 2021; Papangelakis et al., 2022; Ashmore et al., 2023). A threshold between 25 to 40 W/m$^2$ USP has been found by Bizi et al. (2014) to distinguish deposition-dominated reaches and erosion-dominated reaches. The relationship between unit stream power and infrastructure damage has also been studied and a threshold of 300 W/m$^2$ was found to be a triggering point for large-scale geomorphic change to occur and damages to occur to bridges in Vermont, USA (Miller, 1990; Anderson et al., 2017). In Colorado, USA, Yochum et al. (2017) found that the threshold was dependent on slope, with alluvial streams with slopes larger than 3% having a greater capacity to resist geomorphic change. They hypothesized that this was due to armouring of the bed caused by large sediments which creates a diversity of geomorphic units and more stable conditions. Proxies of the gradient of transport capacity such as the gradient in either slope, TSP or USP have been used to estimate the potential of sediments to be transported downstream (Yochum et al., 2017; Sear et al., 2021). Indeed, the gradient of these variables was found in several studies to be useful in determining areas of changes in transport capacity of the river where sediments are expected to deposit (in the case of a negative gradient) or where active erosion can occur (positive gradient) (Beechie & Imaki, 2014; Bizi et al., 2014; Buraas et al., 2014; Bizzi & Lerner, 2015; Gartner et al., 2015; Yochum et al., 2017). Other studies have found contrary results that stream power was not a good predictor of river mobility (Bowman et al., 2021; Parker & Davey, 2023). Therefore, stream power is indeed a useful predictor but must be considered in conjunction with variables at other scales as variables such as the confining material and upstream conditions will also influence the potential for the river to be mobile. (Papangelakis et al., 2022).

6

The geomorphic sensitivity is also dependent on how resistant the landscape is to fluvial erosion (Lisenby et al., 2020). Fluvial forms determined by the extent of confinement and the local confining material can be used to determine a reach's ability to resist change (Lisenby et al., 2020; Beechie & Imaki, 2014; Sear et al., 2021; Wheeler et al., 2022). There exist multiple methods for determining valley confinement, which all attempt to establish the room available for a river to migrate (Beechie & Imaki, 2014; Sear et al., 2021). One method used by Beechie and Imaki (2014) is a confinement ratio calculated as the valley width divided by the bankfull width. This proved to be a simple yet useful ratio to distinguish between confined and unconfined homogeneous reaches but was not useful when incorporated into supervised machine learning techniques to distinguish between braided, anabranching, meandering, or straight reaches (Beechie and Imaki; 2014). In Quebec, the fluvial style has already been assigned to each homogeneous reaches (UEA) within the CRHQ database, while the confinement ratio has not (CEHQ, 2021).

The material of the bed and bank is also important in determining whether or not a river can erode them, with rocky or cohesive soil banks being harder to erode leading to more resistant banks. The erosion of a bank depends on the balance between shear strength and the shear stress, strength being a combination of factors that allow the bank to resist erosion and stress quantifying the amount of erosional force applied to the bank (Simon & Collison, 2002; Rosso et al., 2006). These are influenced by both hydrological and mechanical factors such as the angle of the hillslope, the pore pressure, and the cohesion of the soil (Simon & Collison, 2002). The resistance of the banks to erosion can also be influenced by vegetation growth and therefore the coverage and type of vegetation should be considered when determining the geomorphic sensitivity of a reach (Simon & Collison, 2002; Bywater-Reyes et al., 2022; Ielpi et al., 2022). Vegetation can increase the mechanical strength of the soil by increasing soil tension which makes it more cohesive, with smaller roots increasing the strength more than larger roots (Simon & Collison, 2002). Another way vegetation influences bank strength is by increasing the weight applied on the soil which can increase the friction force making the soil more cohesive. However, this can also have negative impacts on the strength depending on the angle of the slope and placement of the vegetation (Simon & Collison, 2002). Vegetation also impacts the local hydrological processes as the canopy intercepts rainfall and concentrates it around the base of the tree. It also creates negative pressure as it extracts water from the soil for transpiration. These can have both negative and positive impacts on the bank's strength. However, studies show that overall vegetation tends to increase shear strength with grasses being more effective than trees (Simon & Collison, 2002; Ielpi et al., 2022). Bank material and local vegetation can be proxied via publicly available land cover data.

Sediment supply and size of sediments arriving in a reach are important factors in determining whether erosion or deposition will be likely in that reach. If not enough sediments are reaching a reach relative to its transport capacity, then erosion will likely occur, while if the sediments are too large or too numerous they are likely to be deposited (Leopold, 1962; Fryirs & Brierley, 2013; Sear et al., 2021). Currently it is not possible to quantify the total available sediments for a river to transport at large scale, however many proxies exist to estimate the ability of a river to transport sediments and for the size of sediments supplied.

Sediments can be transported from the surrounding landscape into the river during large precipitation events due to landslides or gullying, thus modifying the dynamic equilibrium of the river (Buffin-Bélanger et al., 2015). To estimate the potential for this to occur as well as how far

these sediments could travel an index of connectivity (IC) can be used, acknowledging that the conditions upstream and downstream of sediments entering the river are important in understanding how far those particles could travel (Borselli et al., 2008; Crema & Cavalli, 2018). The distance sediments can travel is important due to sediment sinks such as dams or lakes which can modify the volume of sediments flowing from upstream and therefore modify the dynamic equilibrium (Petts & Gurnell, 2005; Crema & Cavalli, 2018). The IC considers processes impacting sediment transport from local hillslopes into the river as well as along its path in the river such as weir/dam location, slope, drainage area, and land use (Cavalli & Marchi, 2008; Crema & Cavalli, 2018). An open-source software was conveniently developed by Crema & Cavalli (2018) to allow the calculation of the IC with minimal inputs at a high resolution. Sediments can also reach rivers via tributaries, so confluences play an important role in determining the local geomorphic processes (Rice, 1998). However, only tributaries with high sediment loads, and particularly those transporting sediments larger than the main channel, can deposit their sediments at the confluence. In these cases, tributaries may initiate modifications to the local geomorphic units and fluvial form and potentially cause lateral migration downstream (Rice, 1998; Mazgareanu et al., 2020).

The size of the sediment is also important to determine whether a river can transport it, with larger sediments being harder to move than smaller ones. Therefore, watersheds with more fine sediments will tend to have higher volumes of sediment transport (Beechie & Imaki, 2014). The dominating sediment transport mode (suspended or bedload) has also been shown to have an impact on the fluvial style (Beechie & Imaki, 2014; Buffin-Bélanger et al., 2015). Therefore, knowing the size of the sediments upstream of a reach can help predict the fluvial processes that will occur in that reach. In Quebec, many data sets exist to estimate the size and quantity of sediments such as a GIS layers of the morpho-sedimentological zones and surface deposits (Roy & Dion, 2014; Gombault et al., 2022).

### 2.2.2) Other key factors

### 2.2.2.1) Sinuosity

Sinuosity is an important variable when classifying fluvial style as straight or meandering rivers (Beechie & Imaki, 2014). It is calculated as:

$$Sinuosity \ = \ \frac{Reach\ Length}{Straight\ Line\ Length} \tag{2.3}$$

Sinuosity can aid in the prediction of lateral migration with naturally linear channels having less lateral migration than more sinuous channels such as braided or meandering channels (Beechie et al., 2006). In Quebec, the sinuosity of all rivers at the homogeneous reach scale covered by the UEAs have been quantified in an automated manner using the formula above and are publicly available through the CRHQ (MELCC, 2021).

### 2.2.2.2) Large wood and its proxies

Large wood can alter a rivers' geomorphic units and modify sediment transport and erosion processes in certain reaches. However, it is a variable difficult to quantify on a large scale (Ruiz-Villanueva et al., 2016). Depending on the orientation in which it becomes immobilized in a channel, large wood can create pools, meanders, mid-channel bars, or riffles by creating an obstacle for the free flow of sediments and water (Massé & Buffin-Bélanger, 2016; Spreitzer et al., 2021; *Geomorphic Unit Quick Reference Guide*, 2022). These large wood

pileups will frequently be disrupted and transported downstream during large flood events which can cause damage to bridges or culverts (Ruiz-Villanueva et al., 2016).

Proxies have been used to quantify the potential for large wood to be present in a particular river channel such as identifying narrower reaches to identify areas that are prone to large wood becoming immobilized and accumulating (Ruiz-Villanueva et al., 2016). Average upstream width along with average height of trees adjacent to the river was also found to be important in determining the size and volume of large wood that could potentially be transported to the reach (Massé & Buffin-Bélanger, 2016). The size of the catchment can also play a role with medium sized catchments (100 – 1000 km$^2$) transporting more wood than larger or smaller ones (Ruiz-Villanueva et al., 2016). Slope, discharge, and stream power (both TSP and USP) are used to assess the ability of a river to mobilize the large wood. As stream power increases, immobilized large wood becomes less frequent in those reaches (Ruiz-Villanueva et al., 2016).

## 2.3) Influence of anthropogenic modifications on river processes and resulting damage

Several human interventions, mainly occurring in the 20th century, have impacted rivers' dynamic equilibrium (Ashmore et al., 2023). For example, straightening of meandering rivers was common practice in Quebec before being discontinued in the 1980s, but maintenance of these straightened channels is still required to avoid the river migrating again to return to a sinuous pattern (Rousseau and Biron, 2009). Straightening the channel results in steeper slopes, and therefore larger stream power, and thus creates unstable reaches prone to lateral migration and mass wasting (Rousseau and Biron, 2009; Ashmore et al., 2023).

Bank stabilization methods such as riprap are also commonly used to inhibit lateral migration where the local geomorphic variables would naturally cause it, in particular in meandering and wandering rivers and high stream power areas (Russell et al., 2021; Papangelakis et al., 2022). This impedes the dissipation of the stored energy in the discharge and often leads to the displacement of the erosion further downstream as the river continues to build energy without balancing it through sediment transport. A recent study found significant reduction of erosion where the structures were installed but slight increases in erosion downstream when hard structures were used as bank protection (Russell et al., 2021).

Dams also alter the flow of small and large rivers with major consequences on river dynamics downstream (Petts and Gurnell, 2005; Poff, 2014). This is clearly an issue in Quebec with approximately 8500 dams existing in the province (MELCC, 2022). The geomorphic impact of dams can be profound since they alter both the natural flow of water and sediments throughout the river network (Petts & Gurnell, 2005; Poff, 2014). Dams create large sediment sinks inhibiting the free passage of sediments downstream unless they are using specially designed dams to allow these sediments to pass. This disrupts the dynamic equilibrium of rivers and can cause degradation downstream. Dams also regulate discharge and alter or reverse seasonal trends in the river system (Petts & Gurnell, 2005). If the flow permitted to continue downstream is not sufficient it can cause aggradation where tributaries carrying high sediment loads connect to the main channel. Therefore, the impact of dams on river networks is complex and is dependent on the volume of water permitted to exit the dam compared to the sediment load permitted to pass as well as the presence of major tributaries downstream. A general trend was found where if discharge was reduced by less than 10% or increased after building a dam, then degradation occurred while in cases where the discharge was reduced by more than 30% aggradation

occurred (Petts & Gurnell, 2005). The downstream distance potentially affected by dams also varies, with modifications as far as 1 km downstream observed in some rivers while in watershed with many active tributaries the impacts were quickly reduced as the river regained equilibrium between the sediment yield and water discharge due to the sediments from the tributaries (Petts & Gurnell, 2005). It is thus important to consider dams when evaluating the mobility of a reach due it their large impact on the natural river processes.

Bridges and culverts interrupting a channel can cause artificial confinement, a narrowing of the river and changes to the flow due to the pillars of the bridge. This causes an increase in the sediment transport capacity of the river due to forcing the same quantity of water through a narrower channel with no erodible sediments (Ministère des transports, 2019; Wang et al., 2019). The anthropogenic changes related to culverts and bridges can cause scouring beyond the structures due to the increased sediment transport capacity as well as pooling and lateral erosion upstream due to backwater effects if the opening is too narrow for the quantity of water (Brooks and Lawrence, 2000; Wheaton et al, 2015; Wang et al., 2019). Culverts replace a section of river with artificial channels. If these have badly planned slopes, heights, or widths, accumulation can occur within the culvert when slope is too shallow or erosion at the exit when slope is too steep (Ministère des transports, 2019). Roads create artificial confinement of rivers by fragmentating the river valleys with unerodable features, raising the confinement ratio and the cost of bank protection for road safety (Roux et al., 2015).

There are several examples of floods in Quebec that have resulted in major impacts on riverbanks close to bridges. For example, during the 1996 flood in the Saguenay Region, a bridge along the Rivière du Moulin inhibited the flow of the flood resulting in about 20 m of lateral erosion when considering both banks (Brooks and Lawrence, 2000). Scouring along the left bank occurred on the Rivière Chicoutimi where a bridge constricted the flow of water during a flood in a confined valley resulting in the channel incising up to 40 m upstream and 15 m downstream. This large amount of erosion was due to the combination of the artificial confinement caused by the bridge as well as a steepening of the slope of the river which had a non-erodible bedrock riverbed (Brooks and Lawrence, 2000). This scouring caused by changes to the flow by bridges is one of the biggest factors that cause bridges to collapse during large floods (Nasr et al., 2020). A bridge constricting the flow of the river can also result in flood waters overtopping it and flooding the surroundings if the river's banks and bed are non-erodible. This happened during the 1996 Saguenay flood where the water overtopped a bridge in a narrow bedrock gorge causing considerable damage to the local road and some residential buildings (Brooks and Lawrence, 2000).

## 2.4) Machine learning and hydro geomorphological applications

Machine learning (ML) has been increasingly used for hydrological applications and natural hazard detection, although there is a lack of research concentrated on the application of ML for geomorphological applications (Beechie & Imaki, 2014; Wang et al., 2015; Arabameri et al., 2019; Sun & Scanlon, 2019; Sit et al., 2020; Ghosh & Dey, 2021; Gonzales-Inca et al., 2022; Ho & Goethals, 2022; Kavzoglu & Teke, 2022; Avila-Aceves et al., 2023). Two different types of ML models exist which are supervised and unsupervised models, both of which have been applied for hydrological and geomorphological approaches (Beechie & Imaki, 2014; Kasprak et al., 2016; Horacio et al., 2017). Unsupervised methods work by statistically creating clusters of the observations based on how correlated the predictor variables are for those points. These

create groups of observations with similar trends in their variables. This is useful for determining observations with similar conditions, although an analysis is required to determine why these observations were grouped together and what information we can gain from grouping them in this way. This is useful when studying natural trends in the data but does not allow for the prediction of specific user desired classes. Unsupervised models, although less widely used than supervised models for geomorphological applications, have been successfully used to classify homogeneous reaches into categories similar to other classification frameworks and are used to classify rivers globally in the HydroSHEDS hydrological database (Mayer et al., 2014; Kasprak et al., 2016; Horacio et al., 2017; Ouellet Dallaire et al., 2019). The only control the user has on what type of clusters are created during unsupervised classification is the number of clusters, limiting its ability to be used to detect specific trends. The clusters created are also influenced by which clustering algorithm was used and therefore tests should be done to select one based on how the individual predictor variables relate to each other statistically and the intended final clusters (Kasprak et al., 2016; Horacio et al., 2017; Ouellet Dallaire et al., 2019). Figure 2.2 illustrates how the choice of algorithm alters the final clusters and why it is important to test more than one to determine the optimal algorithm for the goal of the project. The individual contribution of each variable in determining which cluster a reference point is assigned to can be determined using principal component analysis (PCA), which allows the interpretation of the clusters and assignment of cluster names relative to the principal variables influencing which observations fall into which cluster (Kasprak et al., 2016; Horacio et al., 2017; Yochum et al., 2017).



A comparison of the clustering algorithms in scikit-learn
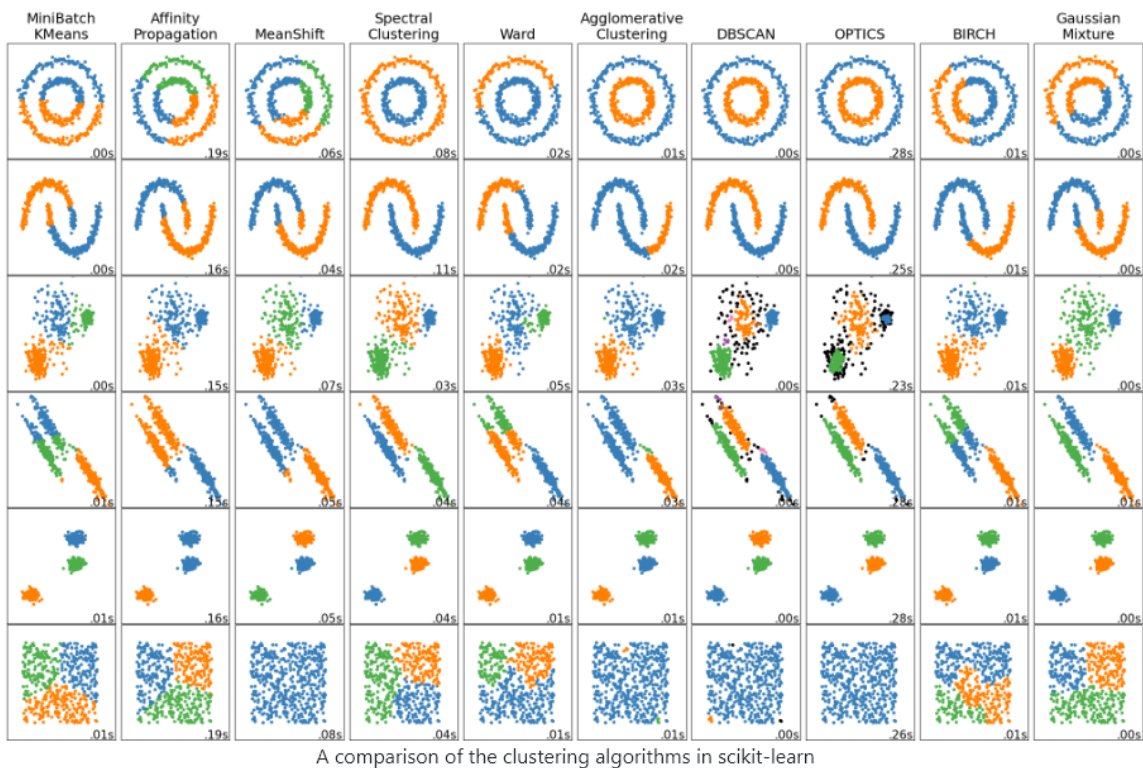
*Figure 2.2: Examples of how clusters created on the same dataset can differ depending on the clustering algorithms used (columns) on 6 different datasets that have different relations between their variables (rows). Taken from the scikit-learn website (https://scikit-learn.org/stable/modules/clustering.html).*

11

Supervised ML models have been used for geomorphic approaches to classify homogenous reaches and geomorphic units as well as detect the potential for natural hazards to occur (Beechie and Imaki, 2014; Arabameri & Pourghasemi, 2019; Gonzales-Inca et al., 2022; Ho & Goethals, 2022). These models work by providing a training dataset in which the desired category to be predicted is associated to a subset of the data that is then used to train a model to detect unique patterns in the predictor variables for each category. This trained model can then be used to predict which category a data point should belong to relative to its values for the predictor variables (Breiman, 2001; Louppe, 2014). One type of supervised model used in the literature is support vector machines (SVM). SVM have been successfully used by Beechie and Imaki (2014) to predict the fluvial styles of homogeneous reaches using channel slope, discharge, valley confinement, sediment supply (mean upstream slope and percent of upstream land in alpine terrain), and sediment size (upstream lithology), these are similar to those that will be used in this study to map the potential of fluvial hazards to occur. Discriminant analysis (DA) has also been successfully used in other geomorphological studies to classify the potential of gullying to occur in certain locations given a set of geomorphic variables (Arabameri & Pourghasemi, 2019). These models have assumptions such as no multicollinearity, independent data, constant variances between groups and normality (Arabameri & Pourghasemi, 2019). These assumptions can often not be met when working with hydrological datasets due to many issues such as spatial autocorrelation, the rarity of some fluvial styles, and collinearity of variables such as slope and USP. The accuracy of the supervised methods will vary depending on how the predictor variables relate to each other and how well the assumptions of the model are met. Therefore, carefully selecting and testing of various models based on their assumptions should be done before choosing the optimal one for the final tool. To determine the best predictor variables and remove excessive predictors, statistical correlation and variable importance tests can be utilized pre- and post-prediction to remove any variables that are strongly correlated with other predictor variables or that are non-significant predictors for any of the clusters (Breiman, 2001; Louppe, 2014).

Among these supervised classification models, there is a subclass of models known as ensemble models (Louppe, 2014). These models use the same methodology as supervised models but create multiple iterations of a supervised model with randomly selected subsets of training data to generate a fixed number of independent supervised models. Ensemble methods have many advantages over other ML methods, such as correcting for imbalances in the training data and noise in the data (Louppe, 2014; Parmar et al., 2019). It is particularly important to correct for these when using ML for hydrogeomorphic applications at large scale. This is because the drainage pattern of each watershed may create conditions that favor one class over another, resulting in an abundance of training points for that class and a lack of training points for other classes (Fairbridge, 2006). It is also beneficial to select a model that corrects for noise in the data that may be prevalent at this scale, as interpretations of where each river hazard begins and ends along a river may differ and variable extraction errors are likely to occur (Parmar et al., 2019).

## 3) Research Objectives

There is a breadth of existing knowledge, tools, and data relevant to river management that can be used to develop tools that can allow a rapid preliminary assessment of the important geomorphic variables at both the local and watershed scale to help river managers or engineers with accurate and cost-effective assessment of river mobility to satisfy the new requirements set

by the Quebec government. The goal of this research is to implement ensemble supervised ML models to identify the dominate fluvial processes of rivers at the watershed scale and display this information in a manner that is comprehensible to an interdisciplinary audience to better incorporate sediment dynamics into Quebec's road infrastructure planning process. Studying the ability of these extracted geomorphic variables to predict the fluvial processes of Quebec's rivers and identify the hazards our road infrastructure is facing can allow for a more sustainable and economical way of planning and maintaining road infrastructure.

The overall objective of this research is therefore to predict susceptibility to fluvial hazards along river networks, with the following two specific research objectives:

**Research Objective 1:** Develop a set of GIS tools to treat data, train ML models, and utilize them to predict the potential fluvial processes occurring in Quebec's rivers. These tools will be specifically designed for datasets available in Quebec to extract the geomorphic variables of rivers and landscapes at large scale and use them to assign points every 100 meters along the river network a value on the susceptibility of the local area to fluvial processes.

**Research Objective 2:** Improve our understanding of which variables are important to consider when predicting the potential for flooding or mobility to occur or when predicting the type of erosion that will occur.

## 4) Methods

The methodology chosen for this study is based on ML models to predict the potential for fluvial hazards to occur. The chosen model is the random forest (RF) classifier model designed by Breiman (2001). Some of the methodology is presented in the next section (manuscript to be submitted to the journal *River Research and Applications*) and is therefore not repeated here. Instead, detailed methodological information not included in the manuscript is provided.

This model was chosen as many studies focused on ML applications for the prediction of natural hazards have shown that it is one of the most accurate models for this purpose (Wang et al., 2015; Ghosh & Dey, 2021; Fang et al., 2022; Hasan et al., 2023; Razavi-Termeh et al., 2023; Youssef et al., 2023). The RF model is an ensemble supervised ML method that classifies the data using decision trees. Therefore, the model will generate a set number of decision trees using random subsets of the user supplied training data to train the models to detect patterns in the variables that allow the classification of the data points into user designated categories. It does this by determining thresholds for the given variables that allow the decision trees to determine a set of these thresholds that allows it to accurate distinguish which user-specified categories should be assigned to each data point. For this study three RF models were trained; a presence of flooding model (PFM) (calibrated to a 20-year recurrence interval), a presence of mobility model (PMM), and a type of erosion model (TEM). For all three models the categories were a binary classification of presence/absence for the PFM and PMM models and for the TEM model the categories were lateral migration or incision. To properly apply ML models to predict the potential for fluvial hazards to occur it was required to extract and prepare predictor variables, create a training/validation dataset, train and calibrate the ML models to use the predictor variables to predict the potential for the fluvial hazards to occur, then validate the accuracy of the models.

13

## 4.1) Data availability in Quebec

Quebec has an abundance of publicly available GIS data that is relevant to hydro geomorphological analyses, and which provide many potential predictor variables (Table 4.1). These datasets contain information on the location and characteristics of the fluvial network, information on the current and future climatic trends, 1-m resolution LiDAR elevation data, as well as land use and surface deposit data. The main dataset used in this study is the CRHQ which contains important information about Quebec's fluvial network. It includes hydrologic, geomorphic, and climatic variables at two scales; the homogenous reach scale, which is segmented based on abrupt changes in variables such as the river slope or different fluvial styles, and the reference points scale with points located every 100 m along the fluvial network (MELCC, 2021).

*Table 4.1: Relevant data available in Quebec*

| Source - Name | Description | Link |
|---|---|---|
| Foret Ouverte – LiDAR | LiDAR covering the majority of southern Quebec (1 m resolution) | https://www.foretouverte.gouv.qc.ca/ |
| CEHQ – Discharge and water levels | Discharge and water level for the gauging stations in Quebec – fairly good coverage in the South, poor coverage in the North | https://www.cehq.gouv.qc.ca/suivihydro/default.asp |
| CRHQ – UEAs/Reference points | Fluvial network containing homogeneous reaches, reference points every 100 meters, fluvial styles, geomorphic variables | https://www.donneesquebec.ca/recherche/dataset/crhq |
| Ouranos – CC data | Multiple models providing current and future climatic variables in raster format covering Quebec | https://www.ouranos.ca/climate-portraits |
| Climate Data Canada | | https://climatedata.ca/variable/ |
| SIGEOM | Geology databases | https://gq.mines.gouv.qc.ca/documents/SIGEOM/TOUTQC/FRA/SHP/ |
| Extracted Variables | Slope ratio, Stream power, Confinement ratio, etc. | Extracted from previous datasets |
| Foret Ouverte - Surface deposits | Surface deposit polygons | https://www.foretouverte.gouv.qc.ca/ |
| IRDA – Surface deposits | | https://geoapp.bibl.ulaval.ca/Home/Index |
| NRCAN – Land cover | 30 m resolution raster land cover for Canada | https://open.canada.ca/data/en/dataset/4e615eae-b90c-420b-adee-2ca35896caf6 |

## 4.2) Predictor variables

From these data sources, 16 variables were extracted that could influence the amplitude and frequency of fluvial hazards which are used as predictor variables. These variables represent processes at multiple scales to allow the model to consider not only the local influences on fluvial hazards but also the potential interaction with the conditions at larger scales such as how it compares to the rest of its homogenous reach or to the conditions upstream of it. The predictor variables are aggregated down to the scale of the reference points every 100 meters, which is the scale at which the final predictions will be made. The majority of the variables used in this study (Table 5.1) were taken directly from the CRHQ, with the exception of the confinement ratio and the discharge used to calculate the unit stream power.

### 4.2.1) Local variables

The main scale of study is the local scale with 11 out of the 16 predictor variables being at this scale. This scale includes variables such as the river slope which is provided in the CRHQ and was extracted from the 1 m LiDAR. The river slope is a crucial variable due to the slope's impact on velocity and therefore on the stream's energy and sediment transport capacity. Therefore, the slope is a good proxy for the local sediment transport capacity but can also be used in the calculation of the unit stream power (USP) which is a direct measurement of the local sediment transport capacity. It can also be used to distinguish certain geomorphic features such as waterfalls and chutes which will have extremely high values of slope relative to the rest of the fluvial network. To compute the USP at each point, the bankfull width and discharge were required. The bankfull width is already included in the CRHQ and was estimated using hydraulic geometry equations based on the drainage area (MELCC, 2021). This provides a rough estimate of the bankfull width, although it fails to take into account the fluctuations in width and potential factors that may influence the river width such as confinement. The CRHQ is currently working on methods to extract the bankfull width from the LiDAR to circumvent these issues and provide more accurate measurements.

For this study the bankfull discharge (Q) is considered equivalent to the 2-years recurrence interval discharge. For reaches with a drainage density above 50 km$^2$ the UEAs already contain discharge values originating from the "Atlas Hydroclimatique" in Quebec which uses a hydrological model (Hydrotel) to predict discharge values using observations from 50 gauging stations to train the model (Direction de l'expertise hydrique, 2018; MELCC, 2021). The CRHQ currently only has discharge values from the Atlas Hydroclimatique 2018, which contains around 5,000 segments, and not those from the most up-to-date version (2022), which contains almost 28,000 segments, including several tributaries. Consequently, a script was created to extract and attach the discharge values from the Atlas to the CRHQ. This script works by providing the Atlas' fluvial network, the CRHQ fluvial network and the 2-year recurrence discharges from the Atlas Hydroclimatique. It then detects the frequency with which each of the individual homogenous reaches of the CRHQ network intersects with a segment of the Atlas Hydroclimatique, and the segment it crosses the most is considered the corresponding segment. Afterwards, it joins the discharge value divided by the drainage area (specific discharge) to the corresponding reach. These values are then joined to the reference points corresponding to that reach and multiplied by the reference point's drainage area. Currently this study is limited to rivers above the 50 km$^2$ threshold. However, for points lower than this threshold, the 2-year

recurrence interval discharge could be estimated using regional power function relationships between discharge and drainage area (DA) of the form:

$$Q = \alpha DA^{\beta} \qquad (4.1)$$

here $\alpha$ and $\beta$ are regional constants (Dunne & Leopold, 1978; Biron et al., 2013). The regional constants for Quebec have been determined by Benyahya et al. (2009). This method is useful in its ease of calculation at large scale, requiring only drainage area measurements easily extractable from a DEM by multiplying the GIS flow accumulation by the pixel area. With access to the local slope, bankfull width, and bankfull discharge the USP was calculated using equation 2.2 in section 2.2.

The CRHQ also provides information on land use near banks, taken from a 2018 study from the Quebec Government at a 10-m resolution (MELCC, 2018; MELCC, 2021). This information was used to create 4 fields reflecting the presence or absence of certain land uses that could impact the hydrological response of the landscape or the stability of the banks. The tools assigned a value of 1 to the corresponding field if wetlands, anthropogenic structures, or farms were present on either bank or 0 if they were not. For presence of vegetation the values ranged from 2 for the presence of high levels of vegetation (forests) on at least one bank, 1 for low levels of vegetation (shrubland), or 0 for an absence of vegetation. This allowed the model to consider any factors that may increase or diminish the potential for fluvial hazards to impact this area such as bank stabilization or vegetation increasing the soil cohesiveness.

At the local level the CRHQ contains the mean angle of deviation between a given reference point and the two adjacent reference points. This variable determines the local curvature of the river, which is useful for determining whether the reference point is at the apex of a meander or in a linear section of the river. This is important for hydro-geomorphological analyses as the apex of meanders tend to be areas of high lateral migration and the most mobile portions of the river. It is therefore useful for determining both the level of mobility and the type of mobility.

The final local variable calculated is the confinement ratio, which is a crucial variable for hydro-geomorphological analyses as the level of confinement and type of confinement material has an influence on both the potential for flooding to occur as well as the level and type of mobility. This variable is not yet included in the CRHQ and therefore needed to be extracted from the LiDAR. To calculate the confinement ratio the bankfull width and the valley width are required. As the bankfull width is already included in the CRHQ only the valley width needed to be extracted from the LiDAR. This was done using Sechu et al.'s (2021) valley bottom detection tool to extract the valley bottom and then a Python script using ESRI tools to determine the width of this valley bottom polygon at every reference point. This tool takes as input data a 10-m DEM, wetlands, the hydrographic network and the watershed boundary. The tool first calculates slopes from the DEM, making sure to replace slope values of zero with a very low value to avoid errors for the next step, which is the calculation by a cost-distance method in which the inputs are slope (without zero values) and the hydrographic network to create an accumulated cost-distance raster file. This cost-distance file represents the distances from any point (pixel) to the nearest river, weighted by the local slope. The tool then uses the cost-distance raster and the potential wetlands to statistically determine a threshold below which values are within the valley, while values above this threshold are outside the valley. By applying this threshold to the cost-

16

distance file, reclassifying the pixels above the threshold to a null value and converting the raster file to a polygon, a valley bottom polygon is created for the river network (Sechu et al., 2021). When using the tools on small (drainage area < 50 km$^2$) and large rivers (drainage area > 50 km$^2$), it is recommended to run them separately for this step, as running them simultaneously may bias the statistical method used to determine the threshold and produce poor results on larger rivers. This consideration is not an issue for the present study, since only rivers with a drainage area >50 km$^2$ have discharge values in the Atlas Hydroclimatique. Comparing the extracted valley bottom results with available hydraulic models, notably the large-scale LISFLOOD-FP model (Choné et al., 2021) generated for the Nicolet and Du Gouffre river basins as part of the INFO-CRUE project (Figure 4.1), we can see that the extracted valley bottom roughly represents the area flooded by a 20-year recurrence flood, which is sufficient to distinguish confined from unconfined rivers (Figure 4.1). Other tools and methods exist to extract this variable, for example Gilbert et al. (2016) "river corridor tools" or VBET ("Valley Bottom Extraction Tool"). However, in the tests carried out during this study, the Sechu et al. (2021) tool proved to be the simplest to use while producing results of sufficient quality to distinguish confinement levels.
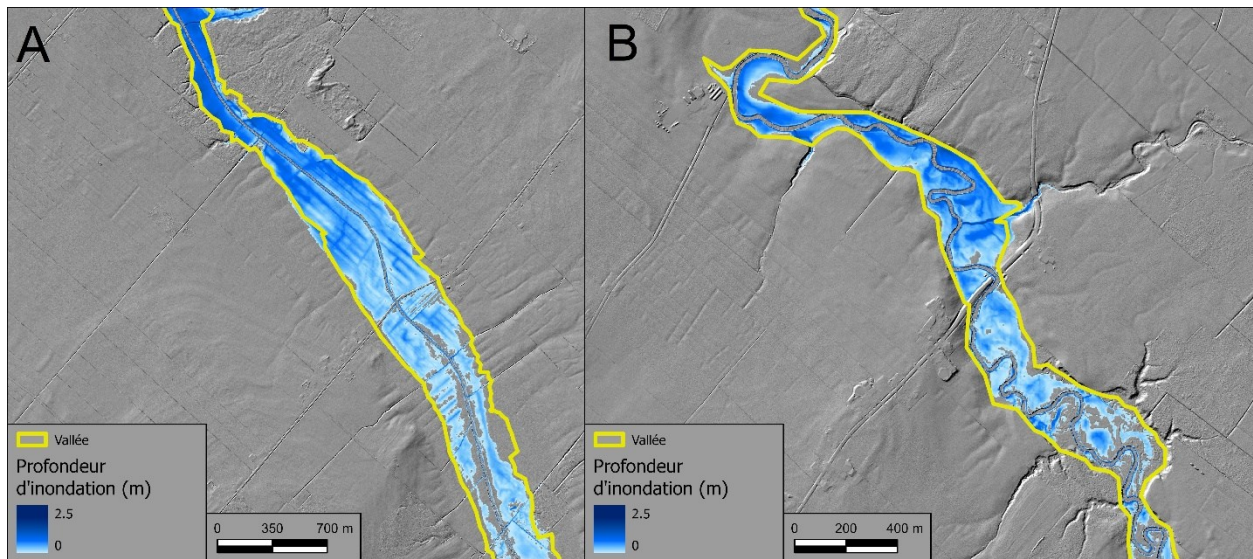


*Figure 4.1: Comparison of the extracted valley bottom polygon with large-scale flood simulations using LISFLOOD-FP based on the methodology of Choné et al. (2021), using a discharge value corresponding to approximately a 20-year recurrence for two rivers in the Nicolet watershed A) Ruisseau Guillemette and B) Laroche river.*

Once computed, the valley bottom polygon is entered into a new tool developed in Python for this project to determine the valley width at each reference point. This new tool takes as input data: the valley bottom polygon, the hydrographic network, and the reference points. This tool then generates transects along the hydrographic network at fixed intervals of 25 m. This threshold has been determined to allow multiple measurements per reference point, so the average is calculated to reduce overestimation errors from badly generated transects. Points are generated in the middle of these new transects, and the transects are clipped using the valley bottom polygon. Points are then generated at the intersection of the transects and the river network, containing the length of the transect. Then, the average of all these intersection points located within 50 m of each reference point is taken and considered as the width of the local valley (Figure 4.2). This method tends to overestimate valley width by around 10% in highly

meandering rivers and at confluences and should therefore only be used to calculate confinement ratios and not for other purposes. It is considered as a temporary solution until CRHQ includes valley width measurements. Estimation of valley width at each reference point is then combined with the CRHQ's estimation of bankfull width to calculate the local confinement ratio.
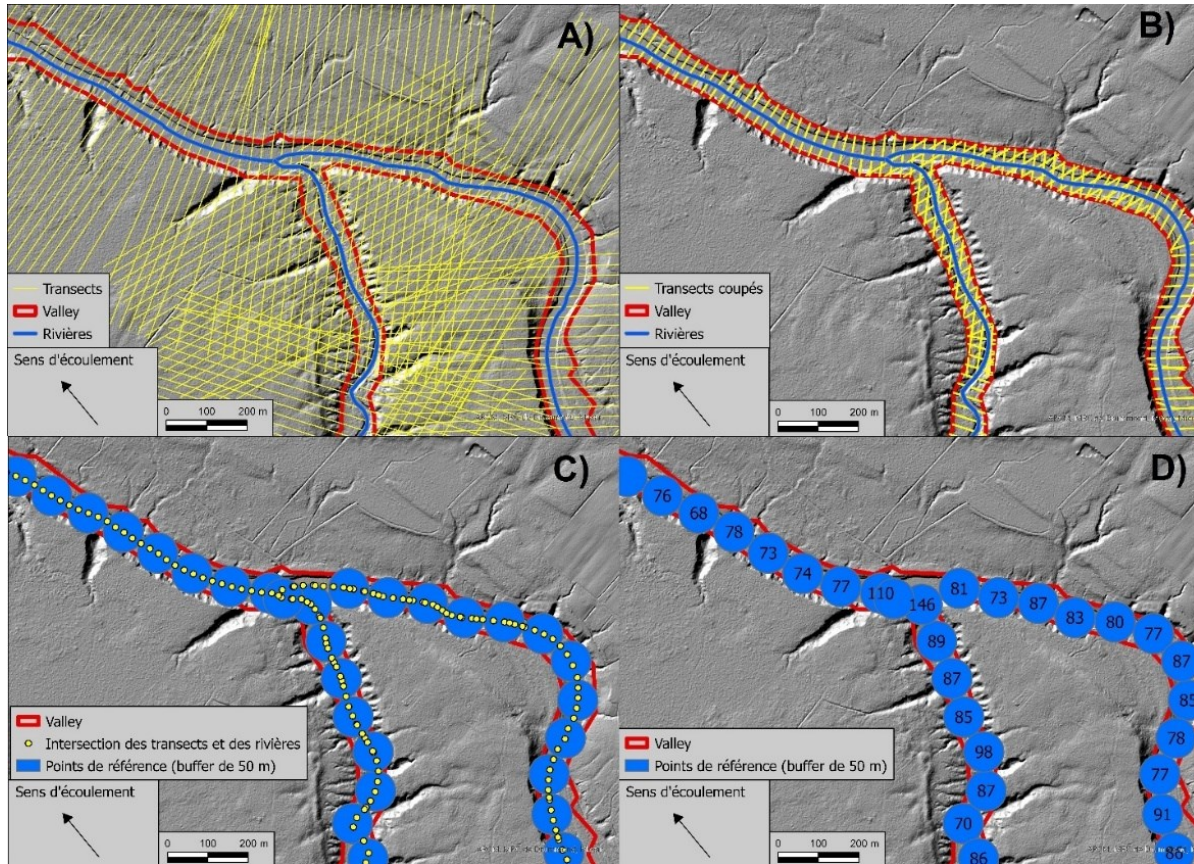


*Figure 4.2: Example of valley width extraction script. A) transects of maximum size generated every 25 m along the fluvial network. B) transects clipped to the extent of the valley. C) intersection of the clipped transects and the river superimposed on the reference points. D) mean valley width at each reference point.*

### 4.2.2) Homogenous reach variables

Two variables quantifying the conditions typical of a homogenous reach were calculated for this study: the mean confinement ratio and the sinuosity of the reach. The mean confinement ratio was calculated by aggregating by mean both the local bankfull width and the valley width for all the reference points in each reach. This provided a mean bankfull width and mean valley width per homogenous reach which was then used to calculate a confinement ratio for the reach. This was also used to calculate the last local variable, the relative confinement, which is the local confinement ratio at each point divided by the homogenous reach's confinement ratio. This is useful for determining areas where the confinement abruptly changes such as in partly confined reaches. The other variable quantified at the homogenous reach level is the sinuosity which is already included in the CRHQ and is useful for determining whether a reach is meandering or linear.

18

### 4.2.3) Watershed variables

As conditions upstream of a point can have an impact on the local fluvial processes by influencing the volume of water and sediments which can reach an area, it was important to include variables that can quantify these processes. Mean upstream slope was used in this study as a proxy for the capacity for upstream sediments to reach a given reference point, with steeper slopes indicating a higher potential for sediments to reach the local area. This is combined with the mean upstream elevation which provides an indication of whether the river is in the headwaters or closer to the mouth of the river. This is a useful indication of the typical type of sediments that will be transported. Finally, the drainage ratio, which is the area of dryland upstream divided by the area covered by water upstream (lakes, dams, rivers), is also considered. This variable is used as a proxy for potential sediment sinks upstream such as lakes or dams that may impact the quantity of sediments that will reach a reference point.

## 4.3) Training/Validation Dataset

To train the models to recognize the patterns in the predictor variables that would allow it to distinguish between given classes and validate that the model is performing well, a subset of the reference points needed to be classified with the desired classes. To classify the reference points, three fields (one for each model) were created and values of 0 or 1 were entered to indicate whether flooding or mobility would occur at this location and whether mobility would be caused by lateral migration or incision (Table 4.2).

*Table 4.2: Classification scheme for the 3 models*

| Value entered | Presence of flooding field | Presence of mobility field | Type of erosion field |
|---|---|---|---|
| 0 | Absence of flooding | Stable | Incision |
| 1 | Presence of flooding | Mobile | Lateral migration |

To classify the reference points four distinct types of data was used: field data collected by the research team as well as by other teams, results from other models/analyses, internal governmental databases, and a hydro-geomorphological assessment based on satellite imagery and LiDAR data (Table 5.2). For field data, we conducted 4 field visits during the summer of 2022; 2 to Nicolet, 1 to Du Gouffre, and 1 to Cascapédia watersheds. During these field visits, information was gathered on the dominant fluvial processes (deposition, erosion, flooding) using evidence such as signs of recent flooding or erosion. We also had access to field data from other studies carried out by Jean-Phillipe Marchand (Ph.D. student in the research lab) in 2009 in the Du Gouffre watershed, as well as by Quebec's government. Results from other models or previous analyses were also used, namely large-scale flood maps generated using LISFLOOD-FP, digitized historical river positions, and results of the channel planform statistic tool (Lauer, 2006). These were only available for the Nicolet and Du Gouffre watersheds. The LISFLOOD-FP results allowed us to calibrate the PFM to detect areas that will likely be flooded during a 20-year flood, while the historical river positions allowed us to identify which sections were most mobile in the last 50 years. For each classified reference point, the final judgement was based on

a hydro-geomorphological assessment using the 1-m LiDAR and satellite imagery to look for signs of recent flooding and erosion following the methodology provided in Biron et al. (2014) and Dupuis et al. (2017).

We also had access to non-public datasets provided by the Quebec's Ministry of Transportation (MTMD) which gave highly relevant information of where road infrastructure was damaged by fluvial processes in the past (Table 4.3). These datasets have been used to complete the training and validation of the model to ensure that the areas where structures have already been damaged are predicted as potentially dangerous zones. The primary internal database used was the "Planification, Programmation, et Suivi" (PPS) which consists of the location, type of work, and reason for the work of all the previously and currently scheduled required infrastructure repairs by the MTMD for the years 1991 to 2023. This dataset was screened for keywords such as "affouillement", "stabilisation," "glissement de terrain," "rivière", "talus," and similar French keywords related to fluvial hazards until satisfied that most of the road works related to these hazards have been identified. The relevant road works was geolocated in the 3 pilot watersheds utilizing the "Base Géographique Routière" (BGR) which consist of the MTMD road network that contains the location of all MTMD managed roads. The "Système de Gestion des Ponceaux et Autres Eléments d'Inventaires" (M012) contains the locations and routine inspection data for culverts. This dataset includes the magnitude of fluvial-related issues such as scouring damaging the extremities of the culvert, infiltration on the outside of the culvert eroding the supporting material, sedimentation and accumulation of wood/debris blocking the culvert, issues with the lateral drainage ditches that drain the groundwater protecting the road from freeze-thaw and infiltration related issues, and changes to the flow of the river due to the culvert. Similarly, the "Système de Gestion des Structures du Québec" (GSQ) contains information for the inspection of bridges and was used to supplement the training/validation dataset. Datasets compiled by regional MTMD authorities relevant to recent fluvial damage to roads available for the Cascapédia watershed was also used to train/validate the model.

*Table 4.3: Internal governmental databases used in project*

| Database | Description |
|---|---|
| Base Géographique Routière (BGR) | Roads managed by the MTMD in Quebec |
| Planification, Programmation, et Suivi (PPS) | Past and current road projects |
| Système de Gestion des Ponceaux et Autres Eléments d'Inventaires (M012) | Past assessments of culvert condition |
| Système de Gestion des Structures du Québec (GSQ) | Bridge location and inspection data |
| Local MTMD databases | Dataset of locations with fluvial related damages to road infrastructure |

# 5) Random forest machine learning models to detect fluvial hazards

This chapter consists of a manuscript that will be submitted to *River Research and Applications* and was written in collaboration with my supervisors Dr. Pascale Biron and Dr. Thomas Buffin-Bélanger. I was responsible for conceptualizing the methodology, collecting the data, organizing the field work, developing the Python tools, training, calibrating, and validating the machine learning models, as well as writing the manuscript. My supervisors provided invaluable support by offering their guidance throughout the process, recommending important readings, revising the manuscript and organization of the administrative portion of the project to secure financing for the project.

## Author names and affiliations

Marco Gava[1], Pascale M. Biron[1], Thomas Buffin-Bélanger[2]

[1]Department of Geography, Planning and Environment, Concordia University
[2]Département de biologie, chimie et géographie, Université du Québec à Rimouski

## Corresponding author

Department of Geography, Planning and Environment, Concordia University, 1455 De Maisonneuve Blvd. W., Montréal, Québec, Canada, H3G 1M8 (M. Gava), M.Gava05@Gmail.com

## Abstract

Fluvial hazards of river mobility and flooding are often problematic for road infrastructure and need to be considered in the planning process. The extent of river and road infrastructure networks and their tendency to be close to each other creates a need to be able to identify the most dangerous areas quickly and cost-effectively. In this study we propose a novel methodology utilizing random forest machine learning methods and hydro geomorphic expertise to provide easily interpretable fine scale fluvial hazard predictions for large fluvial networks. The developed tools provided these predictions at reference points every 100 meters along the fluvial network of three watersheds within the province of Quebec, Canada and used variables focused on river conditions and to proxy hydro geomorphic processes such as sediment transport. Training/validation data was collected in four forms: field data, results from hydraulic and erosion models, government infrastructure databases, and hydro geomorphic evaluations using the 1-m DEM and satellite/historical imagery. First a subset of the reference points was manually classified then divided into training (75%) and validation (25%) datasets. Then the training dataset was used to train supervised random forest models. The validation dataset combined with extensive validation indices indicated the models were capable of accurately predicting the potential for hazards to occur. Metrics are extracted from the model to determine which variables are most important to predict each hazard. Finally, a methodology is proposed for a top-down hazard analysis of extensive fluvial networks to identify the most at-risk infrastructure/communities.

**Keywords**

Fluvial hazards, flooding, erosion, lateral migration, incision, machine learning, random forest

## 5.1) Introduction

Rivers alter their course through the natural fluvial processes of flooding and erosion, both of which provide multiple ecological benefits through the creation of diverse habitats (Florsheim et al, 2008). However, these ecologically beneficial processes create hazards for road infrastructures that cross or are tangential to the river. During flooding events, bridges, road, and culverts can be inundated, blocked by large wood/sediments, or damaged to the point of being unusable (Brooks and Lawrence, 2000; Anderson et al., 2017; Nasr et al., 2019). Often the restriction created by bridges and culverts can increase a floods extent, cause scouring of the riverbed, or initiate erosion of the banks (Brooks and Lawrence, 2000; Anderson et al., 2017; Nasr et al., 2019; Wang et al., 2020). Additionally, normal lateral migration may create instabilities along a road tangent to a dynamic river reach. In many regions, climate change is resulting in increased frequency of large, morphogenetic floods, therefore there is an even higher likelihood of infrastructure being damaged in the future (Nasr et al., 2019). Given the proximity of the road and river networks, it is therefore particularly important to anticipate where in the river network natural flooding and erosion processes may occur, in order to prioritize and plan where and when actions may be required at a regional scale.

Many tools exist to quantify and map the potential for flooding and erosion. However, these tools are often time-consuming and require a great deal of processing power and detailed data. Hydraulic models for example, if properly calibrated, produce highly accurate maps of flood zones, but they require data that are not readily acquirable at large scale such as bathymetry and roughness coefficients (Costabile et al., 2015; Choné et al., 2021). These types of models also require large amounts of manual manipulation of the data, making them expensive to run over large areas (Biron et al., 2014; Costabile et al., 2015), although large-scale flood modelling approaches have been used successfully (Wing et al., 2017; Choné et al., 2021; Avila-Aceves et al., 2023). Alternatively, the hydrogeomorphic cartography approach, which utilizes geomorphic variables as well as evidence of previous flooding and erosion found in satellite imagery, digital elevation models (DEM), and field visits to classify the landscape into landforms (Verstappen, 2011; Biron et al., 2014; Demers et al., 2014; González et al., 2020), is more cost-effective than hydraulic simulations but still requires large amounts of manual digitization. Predictive models for riverbank erosion are usually limited to small reaches (Varouchakis et al., 2016; Saadon et al., 2021) and are often based on digitizing historical river limits using historical imagery to quantify the migration rate of rivers (Winterbottom and Gilvear, 2000; Jautzy et al., 2020). These assessments require a database of historical imagery spanning an appropriate length of time and are resource intensive (Piégay et al. 2005; Biron et al, 2014). Overall, these methods provide accurate results but would be costly to run at the scale of a watershed or of a large territory.

Recently, machine learning (ML) has been increasingly used for hydrological applications and natural hazard detection (Beechie & Imaki, 2014; Wang et al., 2015; Arabameri et al., 2019; Sun & Scanlon, 2019; Sit et al., 2020; Ghosh & Dey, 2021; Gonzales-Inca et al., 2022; Ho & Goethals, 2022; Kavzoglu & Teke, 2022; Avila-Aceves et al., 2023). However, there is a lack of research concentrated on the application of ML for geomorphological applications (Gonzales-Inca et al., 2022). ML methods have several advantages, such as shorter processing

22

times and the fact that no specific variables are needed to run the model, which allows models to be adapted to the available data (Gonzales-Inca et al., 2022). Two main methods exist when applying these models to natural hazards, one storing the variables in rasters and the other in vectors. The raster method is useful for producing results for hazards that affect large areas, such as flooding and landslides (Wang et al., 2015; Arabameri et al., 2019; Mosavi et al., 2020; Ghosh & Dey, 2021; Kavzoglu & Teke, 2022; Avand et al., 2023; Barakat et al., 2023). The vector method is generally used for river classification rather than to detect specific hazards such as river mobility or flooding (Beechie & Imaki, 2014; Guillon et al., 2020; Helm et al., 2020; Buffington & Montgomery, 2022). The vector layer is often a set of homogenous reaches classified into a fluvial style, which could provide information on the potential for fluvial hazards, although to our knowledge no study has attempted to predict the presence of fluvial hazards using this approach (Beechie & Imaki, 2014; Ouellet Dallaire et al., 2019; Sun & Scanlon, 2019; Sit et al., 2020; Buffington & Montgomery, 2022; Gonzales-Inca et al., 2022; Ho & Goethals, 2022). Although it is useful to provide classifications of geomorphic units in rivers, their interpretation requires a specific expertise that is not always available (Buffington & Montgomery, 2022). Both these approaches have their advantages and disadvantages. The raster method provides fine resolution results for the whole territory but requires more processing power and training data in a form that can be converted into a raster layer. The vector method aggregates the surrounding variables to line or point features, which produces less detailed results but requires less processing power, with training data that can easily be modified manually.

This study explores a novel vector ML approach using hydro-geomorphological variables to predict the potential for fluvial hazards to occur at the scale of a vector point file every 100 m over entire watersheds in Quebec (Canada). Rather than classifying river reaches, the prediction of a simple presence/absence with a confidence level for the potential of hazards occurring allows the results to be used by a wide variety of stakeholders who may not have the expertise to interpret geomorphic classification maps. Using reference points every 100 m instead of a raster or the typical homogenous reach method means that a finer scale can be used while keeping the model easy to train and processing times extremely low. The choice of scale was influenced by the availability of the publicly available database called "Cadre de référence hydrologique du Québec" (CRHQ), which includes reference points located every 100 m along river networks in Quebec, with hydrogeomorphic variables attributed to these points (MELCC, 2021). The focus on hydrogeomorphic variables at various scales provide an analysis focused on river processes and hazards with variables similar to other studies that have used a vector method (Beechie & Imaki, 2014; Guillon et al., 2020; Helm et al., 2020). This tool is designed as a preliminary assessment tool to determine locations where more in-depth geomorphological assessments should be undertaken.

## 5.2) Study area and data collection

### 5.2.1) Study Area

This study is located in Quebec, Canada whose landscape was shaped by glacial processes and deposition in post-glacial seas and ice-carved valleys. As a result, river valleys are often made up of deep, easily mobilized glacio-marine till deposited by post-glacial seas such as the Champlain Sea (Dupuis et al., 2017) or of coarse fluvioglacial sediments in confined valleys where local rock outcrops influence lateral and vertical mobility (Marchand et al., 2014).

Three pilot watersheds were chosen to encompass a variety of the geomorphological contexts present in Quebec (Figure 5.1). The Cascapedia watershed is located in the Gaspé peninsula with a drainage area of 3141 km$^2$ and 420 km of rivers, which are predominately confined and incising rivers running through the Appalachian Mountain region (Figure 5.1-A). The mountainous geography of this region makes it difficult to avoid the river network when building infrastructure, which leads to frequent damages to the road network. The Nicolet watershed was selected to represent the St-Lawrence Lowlands region which is one of Québec's most populous regions and consists mainly of glacial and marine sediment deposits (Dupuis et al., 2017). This watershed has a drainage area of 3411 km$^2$, 573 km of rivers, and presents a variety of conditions and fluvial hazards. The rivers originate in the mountainous Appalachian region, with incised confined tributaries flowing into partially confined transition zone rivers before reaching the deep soils deposited by the Champlain Sea in the St Lawrence Lowlands (Figure 5.1-B). The Du Gouffre watershed is located in the Canadian shield region with a drainage area of 999 km$^2$ and 152 km of rivers. This watershed presents a unique context having been highly modified by glacial processes as well as a meteorite impact (Rondot, 2000; Dupuis et al., 2017). The rivers originate in the mountainous region with high slopes quickly draining into the mobile, partly confined, Du Gouffre River (Figure 5.1-C). Note that within these three networks, only rivers with drainage areas larger than 50 km$^2$ were included in the study as discharge data were not available for smaller rivers.
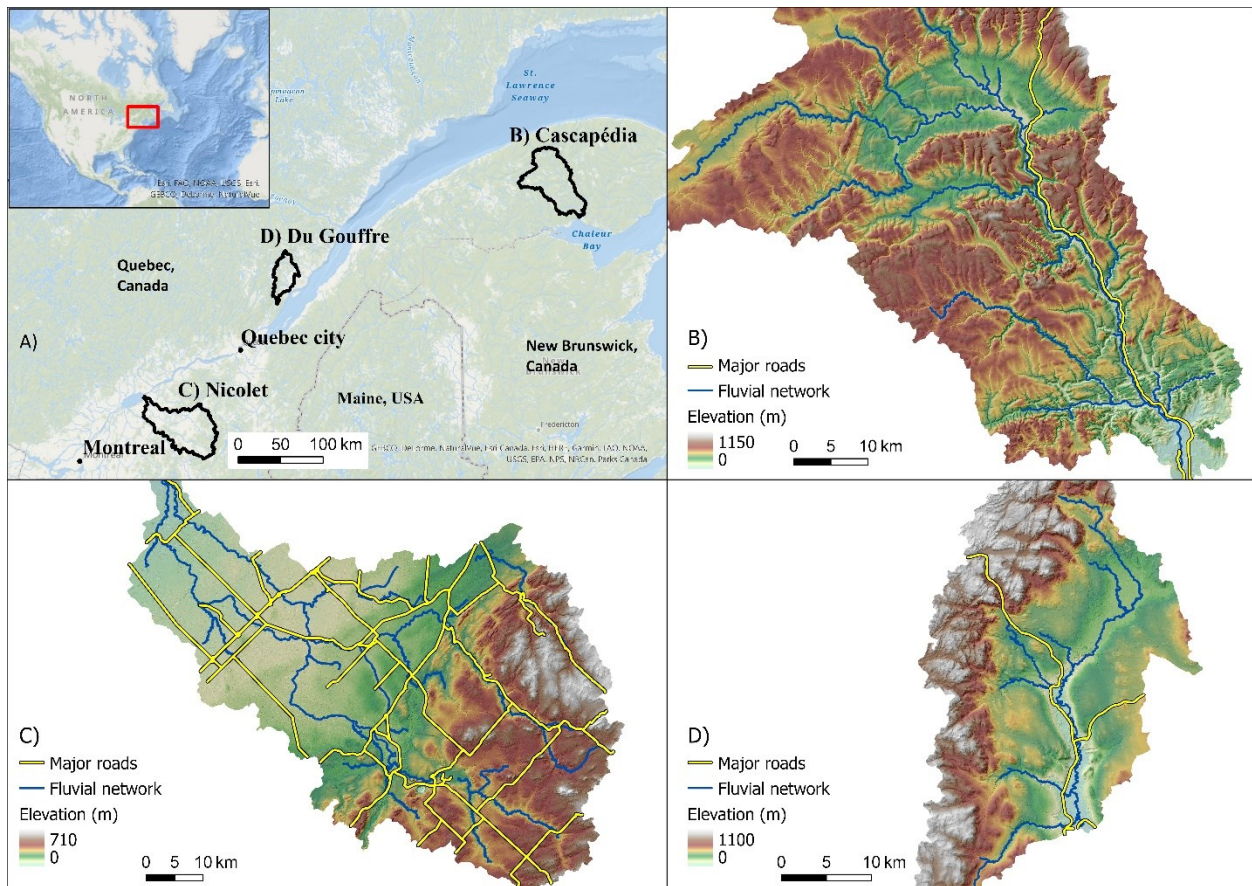


*Figure 5.1: A) Location map of the pilot watersheds in Quebec: B) Cascapédia; C) Nicolet, D) Du Gouffre. The major rivers (drainage area > 50 km$^2$) and major roads (only those managed by the provincial government are presented.*

24

**5.2.2) Geomorphic data collection**

The southern part of Quebec (where the majority of the population lives) is fully covered with publicly available LiDAR (Light Detection And Ranging) high-resolution (1 m) DEM data. The CRHQ, which is the main dataset used in this study, includes the river network/reference points as well as several hydro-geomorphological variables related to fluvial dynamics, including some extracted from the LiDAR datasets. It stores these variables at two scales, the homogeneous reach scale, called "Unité Écologique Aquatique" (UEA), which uses variables such as river slope, unit stream power and sinuosity to delimit reaches, and reference points located every 100 m along the river network. These reference points will form the scale at which the model will be trained and the results generated.

The CRHQ dataset is still being developed in Quebec, so some key variables are missing that should be incorporated in the coming years. One of these missing variables is local confinement, which is a key variable in flood and erosion prediction, as geologically confined rivers are limited in their ability to flood their surroundings or erode their banks (Beechie & Imaki, 2014; Demers et al., 2014; Fryirs et al., 2016; Fryirs & Brierley, 2018; Wheeler et al., 2022). The width of the confining valley was extracted from the 1-m DEM using a Python script combining the river valley bottom detection tool of Sechu et al. (2021) with ESRI Arcpy tools to generate transects along the river network, clip them to the valley bottom, and aggregate the mean length of these transects in 50 m buffers around each reference point. Three confinement ratios using the formula of Beechie & Imaki (2013) were calculated by combining the extracted local valley width and the river width from the CRHQ (determined using hydraulic geometry). The three ratios are local confinement, mean confinement of homogenous reaches, as well as relative confinement:

$$Local\ confinement\ ratio = \frac{Valley\ width}{Bankfull\ width} \tag{5.1}$$

$$Reach\ confinement\ ratio = \frac{Mean\ valley\ width\ of\ the\ homogeneous\ reach}{Mean\ bankfull\ width\ of\ the\ homogeneous\ reach} \tag{5.2}$$

$$Relative\ confinement\ ratio = \frac{Local\ confinement\ ratio}{Reach\ confinement\ ratio} \tag{5.3}$$

The relative confinement ratio is an index that can be used to determine whether the local reference point is located in an area that is more or less confined than the rest of its homogenous reach. It is useful in environments with partly confined rivers in which the dominating local fluvial processes may vary depending on the confinement levels.

The CRHQ database includes bankfull discharge information, assumed equivalent to a 2-year recurrence discharge, based on hydrological modelling done for the province of Quebec ("Atlas Hydroclimatique du Québec meridional", https://www.cehq.gouv.qc.ca/atlas-hydroclimatique/index.htm). This is used to compute unit stream power at each reference point. A total of 16 variables were extracted from the CRHQ database and the in-house confinement GIS tools at 3 different scales (local, homogenous reach, and watershed) (Table 5.1).

*Table 5.1: List of variables used during the study.*

| Scale | Variable | Units |
|---|---|---|
| Local | Local slope | m/m |
| | Mean angle between current point and adjacent points | degrees |
| | Channel width | m |
| | Drainage area | $km^2$ |
| | Unit stream power (USP) | $W/m^2$ |
| | Presence of agricultural land on the banks | Presence (1)/absence (0) |
| | Presence of wetlands on the banks | Presence (1)/absence (0) |
| | Presence of vegetation on the banks | Presence (1)/absence (0) |
| | Presence of anthropogenic features (city, road, bridge) on the banks | Presence (1)/absence (0) |
| | Local confinement ratio | m/m |
| | Local confinement ratio relative to its reach's confinement ratio | - |
| Reach | Mean confinement ratio for the reach | m/m |
| | Length of reach divided by straight line distance of reach | m/m |
| Watershed | Mean slope upstream of point | % |
| | Mean altitude upstream of point | m |
| | Upstream dryland area divided by upstream wetted area | $m^2/m^2$ |

## 5.2.3) Training and validation data collection

A subset of the reference points needed to be classified with information on flooding and erosion to train and validate the models. Three random forest (RF) models were developed in this study, namely 1) the presence of flooding model (PFM), based on a 20-year recurrence flood, 2) the presence of mobility model (PMM), detecting mobility that could justify a more detailed study, and 3) the type of erosion model (TEM), which distinguishes incision or lateral migration for cases where river erosion is expected. Several datasets and methods were used to classify these points, the main method being hydro-geomorphological mapping in which 1-m LiDAR DEM, satellite imagery and historical aerial photographs were used to assess the potential occurrence of these fluvial hazards (Biron et al., 2014). To ensure the classification was accurate various validation datasets were collected. They included field observations collected during this study as well as some from previous studies, results from various models looking at flooding (e.g. large-scale model LISFLOOD-FP (Choné et al., 2021) on the Nicolet and Du Gouffre Rivers) or river mobility Channel planform statistics toolbox (Lauer, 2006) on the Du Gouffre

River, freedom space maps (Biron et al., 2014) on parts of the Nicolet River), as well as government datasets on previous fluvial-related damages to road infrastructure (Tables 5.2 and 4.3).

*Table 5.2: Types and description of the data used to train and validate the random forest models.*

| Types of data | Description |
|---|---|
| Field data | 1.      Observations of bank stability in the Du Gouffre watershed collected in 2009 by Concordia<br><br>2.      Photos and observations collected by the authors during summer and fall 2022 (all watersheds)<br><br>3.      Field data collected by the Ministry of Environment of Quebec (MELCCFP) in the Gouffre watershed in 2022. |
| Channel Planform statistics toolbox model results | Model predicting bank erosion rates for the Du Gouffre watershed using historical river alignments for a 56-year period (2020 vs. 1964) |
| LiDAR | Use of high-resolution DEM to identify evidence of past and present flooding/erosion, such as flood scars and former bank failures and landslides |
| Historical photos | Comparison of historical photos dating back several years to identify where the river has migrated and determine whether this was an abrupt or gradual change. |
| Satellite imagery | Assessment of modern satellite imagery for signs of riverbank erosion, such as the absence of vegetation or landslide failures. |
| Internal Ministry of Transportation of Quebec database | Road infrastructure (roads, bridges, and culverts) inspection data and repair logs. |

For the three pilot watersheds, a total of 1,807 points were classified for flooding, 1,542 for mobility, and 847 for the type of erosion out of the 11,452 reference points for the 1,145 km of rivers included in the study, which represents between 7% to 16% of the total points being classified according to the model. Flooding is easier to identify using LiDAR and large-scale modelling results (Choné et al., 2021; 2022), which explains the higher number of points classified for this hazard. On the other hand, the higher number of points for mobility compared to erosion type is explained by the fact that stable areas are not considered in the erosion type

model, which aims to distinguish between the dominant river process causing the mobility (incision or lateral migration). The number of reference points classified for each category in the models for the presence of flooding and the presence of mobility were well balanced with a difference of 29% and 22% respectively between the presence and absence classes of the two models with the presence class having more classified point in both cases. However, incision is more difficult to identify than lateral migration and is also more likely to occur in small headwater streams that were not included in this study which focused on rivers with a drainage area of 50 km$^2$ or more. Therefore, there are more points classified for lateral migration than for incision, with 72% of the classified points being for the lateral migration class. This may cause issues of the model becoming overtrained at detecting lateral migration relative to its ability to detect incision.

## 5.3) Machine learning methodology

### 5.3.1) Random forest

There are several types of supervised ML models, each with its own advantages and limitations. For this study the random forest classifier model (RF) designed by Breiman (2001) was chosen as a large number of studies focused on natural hazards have shown that it is one of the most useful ML models for predicting flooding and erosion (Wang et al., 2015; Ghosh & Dey, 2021; Fang et al., 2022; Hasan et al., 2023; Razavi-Termeh et al., 2023; Youssef et al., 2023). These models were trained utilizing the Scikit-learn Python API (Pedregosa et al., 2011; Buitinck et al., 2013). This is an ensemble supervised model that consists of multiple decision trees (representing a forest), where each tree corresponds to a vote and the final prediction depends on the total number of votes (Breiman, 2001; Fang et al., 2022). It uses subsets of user-supplied training data to predict user-supplied classes, which in this study are absence/presence of flooding (PFM) or mobility (PMM), as well as the type of erosion (lateral migration or incision, TEM). A subset of the reference points containing both the geomorphological variables and associated classes to be predicted for the three models was subdivided into a training and validation dataset. The training dataset, which comprises 75% of the classified data, is used by the models to determine the patterns of available geomorphologic variables that allow the models to predict which class should be associated with that combination of geomorphological variables. The validation dataset, which comprises the remaining 25% of the classified data, is then used to validate the model's performance on data on which it has not been trained.

The RF method has many advantages over other ML methods, such as correcting for imbalances in the training data and noise in the data (Parmar et al., 2019). It is particularly important to correct for these when using ML for hydrogeomorphic applications at large scale. This is because the geomorphic context of each watershed may create conditions that favor one class over another, resulting in an abundance of training points for that class and a lack of training points for other classes. Since the tool is aimed to predict flooding and mobility at reference points every 100 m for a very large territory (here, three pilot watersheds, but ultimately the entire province), it is also beneficial to select a model that corrects for noise in the data that may be prevalent at this scale, as interpretations of where each river hazard begins and ends along a river may differ and variable extraction errors are likely to occur.

### 5.3.2) Collinearity

When using ML methods, it is important to test the correlations between variables, as variables that are not independent of each other or that are too correlated can cause problems when interpreting the results of the model (Kavzoglu & Teke, 2022; Tiwari, 2022). In effect, the importance of certain variables is artificially increased by giving the model essentially the same variable twice, which also reduces the importance of other variables that may be more important than they appear if collinear variables are added to the model. To test for correlation, the Spearman's rank correlation was computed and then converted to a distance matrix to calculate Ward's clustering method to create a dendrogram of the most correlated variables (Spearman, 1904; Ward, 1963; Daniel, 1990; Tien Bui et al., 2016; Vasu & Lee, 2016; Guillon et al., 2020). A threshold of 0.25 was chosen to create groups of variables. If the correlation between two variables was below this threshold, one of them was removed.

### 5.3.3) Model calibration

The RF model has two main parameters to calibrate: the number of trees generated (an integer value) and when the trees should stop creating new nodes (Parmar et al., 2019; Fang et al., 2022; Scikit-learn developers, 2023). Controlling when the trees should stop generating new nodes can be done using different techniques. Here, it was calibrated by entering a percentage of the total training database to determine the minimum amount of data points per final node (Scikit-learn developers, 2023). The values used for the percentage of the training database to determine the final node ranged from 0.25% to 10% to determine the minimum number of data points per node. To calibrate the models, the accuracy of the models on the training and validation data was plotted against the number of decision trees and the percentage of training data used as the minimum number of points per final node.

### 5.3.4) Validation Indices

To validate the models, common validation indices from random forest models on natural hazards were used. These include a confusion matrix containing the values correctly predicted (true negatives/positives, TN/TP) and the values incorrectly predicted (false negatives/positives, FN/FP), these were used to calculate the individual precision for each class ($P_X$), accuracy of the model ($P_t$), recall (R), specificity (S), Kappa coefficient (K), and F1-scores (Fang et al., 2022; Kavzoglu & Teke, 2022; Tiwari, 2022; Avand et al., 2023; Youssef et al., 2023). As the models are limited to binary classifications the area under the curve (AUC) of the receiver operator characteristic graph (ROC) was also used (Tiwari, 2022). The ROC is a graph of recall versus the false positive rate (FPR) with varying thresholds of votes needed to be classified as the true class (presence of hazard in our study). The AUC is calculated for this graph and is used as a metric to evaluate a model's performance. As the random forest model used is the classifier model and not the regression model the root mean square error (RMSE) and similar indices were not included. It is also important to ensure that the model is not over-fitted to the training data as this would compromise its ability to predict hazards in hard-to-reach areas where it would be difficult to collect training/validation data or in watersheds it has not yet been trained on. In this study over-fitting was quantified as the difference between the accuracy of the model when used on the training data relative to when it is used on the validation data.

$$Precision = \frac{TX}{(TX+FX)} \quad (X = positive\ (P)\ or\ negative\ (N)) \quad\quad (5.4)$$

$$Accuracy = \frac{(TN + TP)}{(TN+TP+FN+FP)} \tag{5.5}$$

$$Recall = \frac{TP}{TP+FN} \tag{5.6}$$

$$Specificity = \frac{TN}{TN+FP} \tag{5.7}$$

$$Kappa\ coefficient = \frac{2*(TP*TN-FN*FP)}{(TP+FP)*(FP+TN)+(TP+FN)*(FN+TN)} \tag{5.8}$$

$$F1-score = 2 * \frac{A*R}{A+R} \tag{5.9}$$

$$False\ positive\ rate = \frac{FP}{TN+FP} \tag{5.10}$$

$$Overfitting = A_{validation\ data} - A_{training\ data} \tag{5.11}$$

To test the importance of the variables for the model two indices were used, MDI and the MDA (Breiman, 2001; Louppe, 2014; Nembrini et al., 2018). When using these indices, it is important to consider that continuous variables will have higher values than discrete variables (Nembrini et al., 2018). The MDI quantifies by how much the GINI impurity of nodes was reduced when split by that variable on average (Louppe, 2014). The GINI impurity is a metric used in decision trees to determine what is the probability that a random data point selected from a node within the decision tree will have the incorrect class (Louppe, 2014). Therefore, higher MDI scores signifies that the variable was useful in differentiating between the presence or absence of fluvial hazards. The mean decrease in accuracy works by generating multiple iterations of predictions while randomly shuffling a target variable and quantifying on average by how much the accuracy of the model decreases (Breiman, 2001; Nembrini et al., 2018). If a variable has a high MDA value, it means that it is an important variable to accurately predict the presence or absence of hazards (Nembrini et al., 2018).

$$GINI\ Impurity\ (I) = 1 - Prob(correct\ prediction)^2 - Prob(wrong\ prediction)^2 \tag{5.12}$$

$$MDA = 1 - \frac{1}{n}\sum_{1}^{n} Model\ accuracy\ with\ randomized\ variable \tag{5.13}$$

### 5.3.5) Confidence level

For the RF model it is possible to assess the confidence of the prediction at each reference point by the number of decision trees that voted for a given class relative to the total number of decision trees generated within the RF model. Since the models were trained using 100 trees, the confidence interval is the number of models out of 100 that voted for a class, with 50% being the lowest possible value, indicating that the model was not able to determine with certainty which class (presence or absence) to predict for that location, as there is 50% of the trees that voted for that class and therefore 50% also voted for the other class.

To facilitate analysis and interpretation of the results by a wide range of experts, easy-to-interpret susceptibility categories have been created using confidence levels where thresholds have been determined using approximately one standard deviation from the mean of the

30

confidence levels for each model, giving the following thresholds: less than or equal to 55% for uncertain, between 56 and 75% for medium certainty, and greater than 75% for high certainty.

## 5.4) Results

### 5.4.1) Collinearity and calibration

The collinearity analysis revealed that there were four cases of variables from Table 5.1 that were too collinear. First, river channel width is very strongly correlated with drainage area, because in the CRHQ dataset, width is estimated as a function of drainage area (hydraulic geometry relationship). This will change in future versions of CRHQ, as a new method of determining width from LiDAR is currently being developed. Since width is used in the calculation of unit stream power (USP, proportional to the product of discharge and river slope divided by width, equation 2), it was removed from the model and the drainage area was retained. The local river slope and USP are also highly correlated since river slope is used to calculate USP. The USP was retained to incorporate the local width and river slope into the model. The third case is the local and valley confinement ratios, which was expected since the valley confinement ratio is the average confinement ratio of all local measurements within a homogeneous reach. The local value was retained because the model also includes the relative confinement, which measures whether the confinement of the homogeneous reach is larger or smaller than the local confinement. Finally, the average river slope upstream and average elevation upstream of the local point are correlated with each other, which is probably explained by the fact that headwater streams tend to have steeper slopes and that, consequently, the higher the mean elevation upstream, the steeper the slope is likely to be upstream. The upstream slope is a better indicator for estimating the amount and type of sediment likely to reach the local area, as it remains more constant between watersheds in relation to elevation and was therefore retained to allow the model to be used on other watersheds that may have different ranges of elevation. The variables that were removed and remaining variables are reported in table 5.3.

*Table 5.3: Remaining variables after collinearity analysis*

| Scale | Variable | Units |
|-------|----------|-------|
| Local | ~~Local slope~~ | ~~m/m~~ |
| | Mean angle between current point and adjacent points | degrees |
| | ~~Channel width~~ | ~~m~~ |
| | Drainage area | km$^2$ |
| | Unit stream power (USP) | W/m$^2$ |
| | Presence of agricultural land on the banks | Presence (1)/absence (0) |
| | Presence of wetlands on the banks | Presence (1)/absence (0) |
| | Presence of vegetation on the banks | Presence (1)/absence (0) |
| | Presence of anthropogenic features (city, road, bridge) on the banks | Presence (1)/absence (0) |
| | Local confinement ratio | m/m |

| | Local confinement ratio relative to its reach's confinement ratio | - |
|---|---|---|
| Reach | ~~Mean confinement ratio for the reach~~ | ~~m/m~~ |
| | Length of reach divided by straight line distance of reach | m/m |
| Watershed | Mean slope upstream of point | % |
| | ~~Mean altitude upstream of point~~ | ~~m~~ |
| | Upstream dryland area divided by upstream wetted area | $m^2/m^2$ |

When calibrating the number of trees, it was found that increasing the number of trees did not significantly improve the accuracy of the model but increased the processing power (Figure 5.2-A). Therefore, the default value of 100 trees was selected. This is contrary to Wang et al. (2015) and Fang et al. (2022) which both used a raster method and found modifying the number of trees had an impact on the accuracy of their model. They found 10 000 and 200 trees to be the best number of trees respectively which would increase processing time significantly relative to the 100 trees used in this study. Fang et al. (2022) noted that going from 100 to 200 trees increased processing time by 62.5%, illustrating a potential advantage of using the less computationally and data intensive vector approach over using raster data. Modifying the parameter indicating when to stop generating new decision tree nodes had a much larger impact on the accuracy with a 10% difference when using 0.25% relative to 10% of the training data (Figure 5.2-B). This value is also important to calibrate as it controls the level of over-training, which results from splitting the decision trees dividing until each node contains only a very small number of datapoints resulting in a model that is well trained to predict the points it has been trained on, but not the points it has not been trained on. This can be seen by comparing the precision of the model using the training data with that using the validation data. Figure 5.2-B highlights how increasing the minimum number of data points per node reduces the over-training of the models, although it does also reduce the overall accuracy of the model. It is important to select a threshold that both minimizes over-training while maintaining a high accuracy value. A threshold of 2% was chosen for the three models, as it resulted in the highest accuracy while

minimizing the difference between the accuracy of the training and validation data.
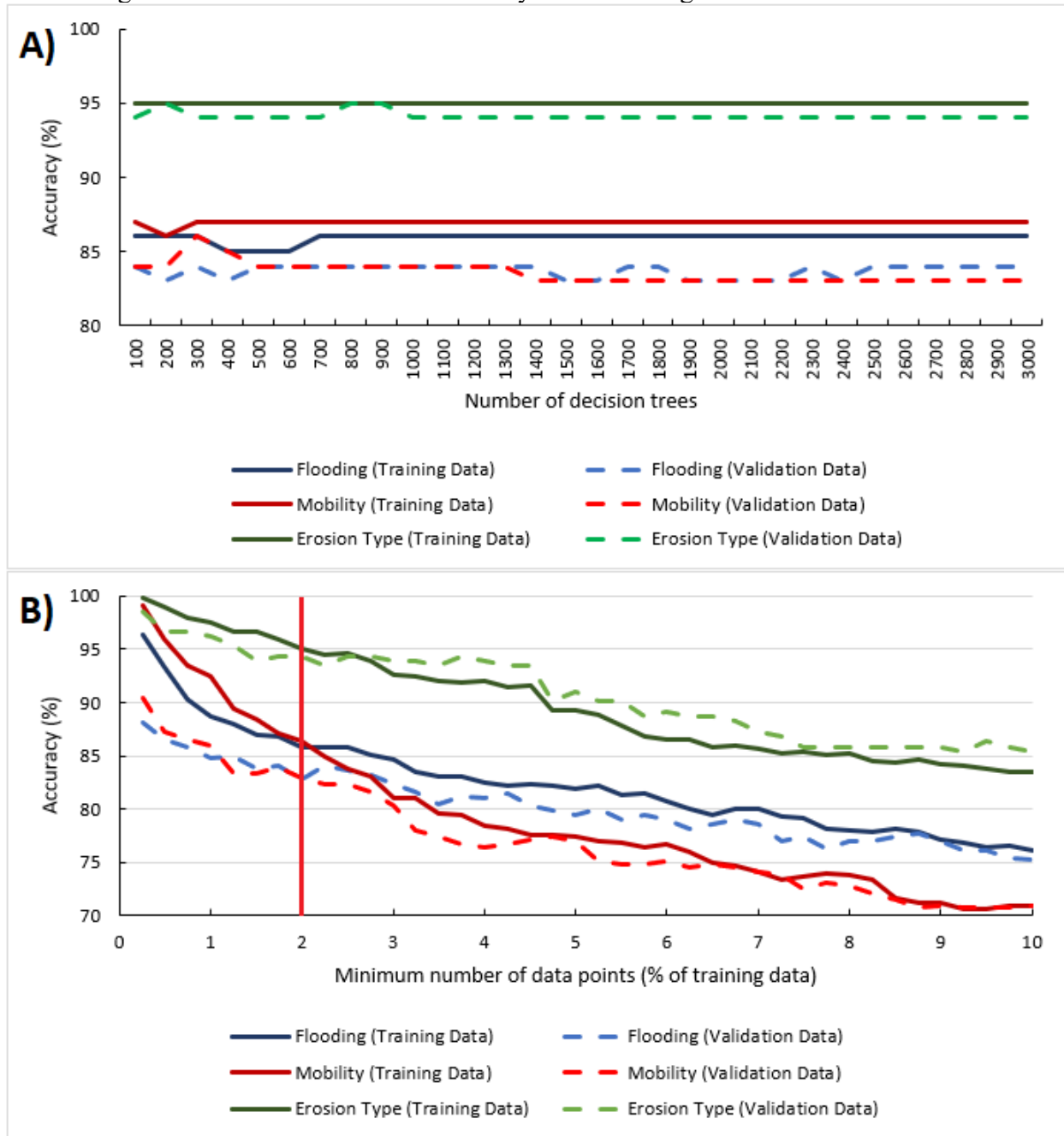


*Figure 5.2: Calibration results for the three models showing model accuracy against the number of decision trees (A) and the minimum number of data points per final node as a function of a percentage of the training data (B).*

## 5.4.2) Predictions for the pilot watersheds

Figure 5.3 presents the results for the three models for the three pilot watersheds (column A – flooding, B – mobility, and C – type of erosion). At the watershed scale used in Figure 5.3,

33

the heterogeneity of the predictions every 100 m along the river network is not clearly visible, with several overlapping points.

The PMM model predicted that 44.5%, 82.0%, and 68.3% of the river network was mobile for the Nicolet, Cascapédia, and Du Gouffre watersheds, respectively. These results were expected because the topography of the Cascapédia region favours the mobility of rivers, which are limited to narrow floodplains confined by mountains rising on average around 200 m above the river. This results in a high diversity of fluvial processes due to faster velocities combined with a higher diversity of sediment types. However, there is a lack of training data in these types of streams due to the remoteness and lack of roads to access these rivers, so the heterogeneity of processes occurring in these streams is not correctly predicted by the model. For the other two watersheds, the results are in line with expectations. The Du Gouffre watershed showed incision in the high-energy tributaries and lateral migration (or stable reaches) in the partially confined Du Gouffre main river. In the Nicolet watershed, there is mobility in the higher-energy portions in the Appalachian region in the southeast of the watershed, more stability in the center and mobility near the confluence between the Nicolet River and the St. Lawrence River. For flooding the results were 48.9%, 53.3%, and 44.0% of the network being at-risk for the Nicolet, Cascapédia, and Du Gouffre, respectively. These results are expected as the geomorphic history and topography of these watersheds limits flooding in many areas due to geological confinement or the river which is incised in glacio-marine till, resulting in high banks that are still erodible but that limit flooding. Given that the study focused on large rivers and the lack of training data for incision, only 10.2% of the mobile points in the Nicolet and 22.0% of the mobile points in the Du Gouffre and Cascapédia were predicted as incision.
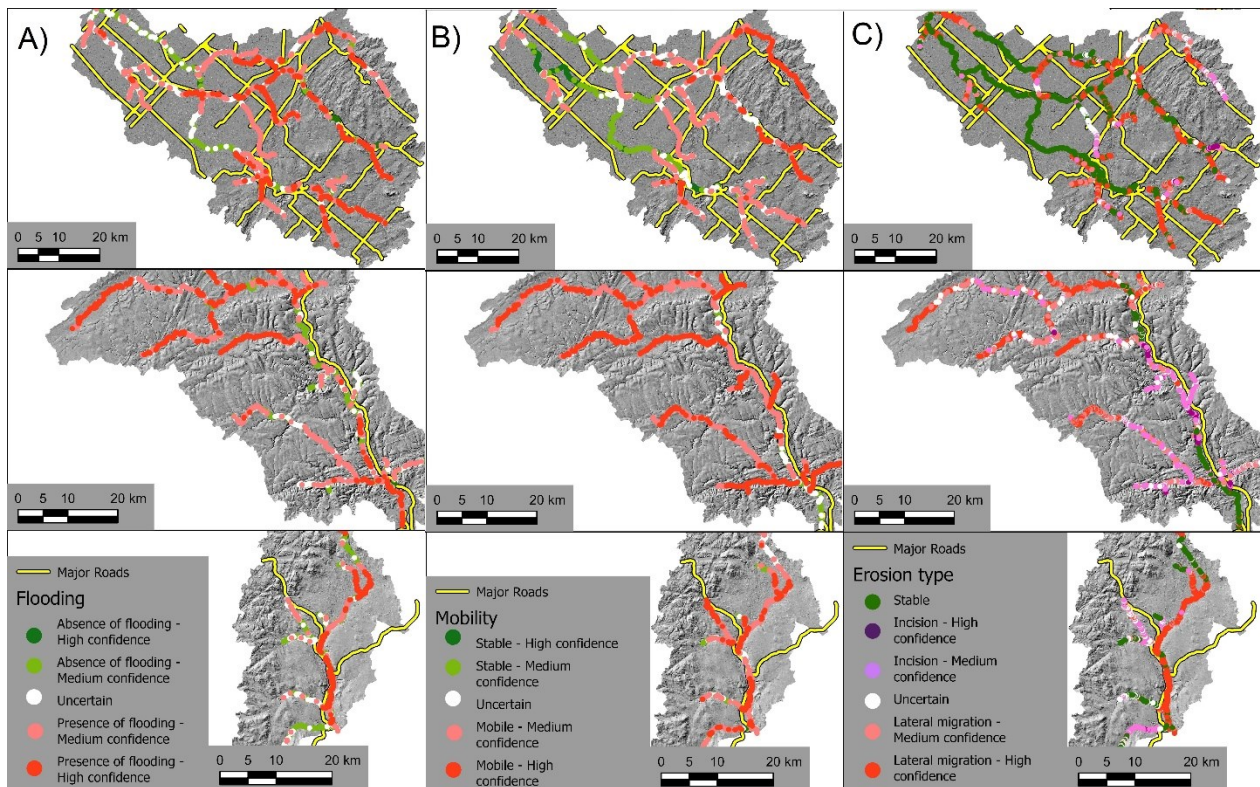


*Figure 5.3: Overview of predictions and confidence levels for A) the presence of flooding, B) presence of mobility, and C) type of erosion models for the three pilot watersheds: Nicolet (top row), Cascapédia,(middle row) and Du Gouffre (bottom row).*

34

When evaluating the three models' accuracy on the validation data for the three pilot watersheds, 83%, 83%, and 94% of the points were correctly predicted by the PFM, PMM and TEM, respectively (Table 5.4). Table 5.4 also reveals that the levels of over-training were very small, with at most a 3.5% difference between the training and validation accuracies. More importantly, it reveals that the recall (R) is high, which is important for a study on fluvial hazards as predicting a hazardous area as safe could have disastrous consequences. The PFM and PMM models are accurately predicting 86% and 90% of the hazardous areas, respectively, which, based on other ML models to detect natural hazards (Fang et al., 2022; Kavzoglu & Teke, 2022; Avand et al., 2023; Youssef et al., 2023) is considered very good to excellent. The other variables used to compare ML models such as the F1 score, kappa, and AUC also rank them into these categories. The model was also validated using only the accuracy measure for a watershed (Coaticook) it was not trained on (details on this analysis can be found in appendix A).

*Table 5.4: Confusion matrix and validation indices for each model (S = specificity, R = recall, and A = accuracy).*

| A) | | Flooding | | |
|---|---|---|---|---|
| | | Observations | | |
| | | Absence | Presence | Precision |
| Predictions | Absence | 155 | 36 | 81% |
| | Presence | 42 | 219 | 84% |
| | S/R/A | S = 79% | R = 86% | A = 83% |
| F1 Score | 84.5% | | | |
| Kappa | 64.8% | | | |
| AUC | 90% | | | |
| Over-fitting | 3.1% | | | |
| B) | | Mobility | | |
| | | Observations | | |
| | | Absence | Presence | Precision |
| Predictions | Absence | 120 | 22 | 85% |
| | Presence | 44 | 200 | 82% |
| | S/R/A | S = 73% | R = 90% | A = 83% |
| F1 Score | 86.4% | | | |
| Kappa | 64.4% | | | |
| AUC | 90% | | | |
| Over-fitting | 3.5% | | | |
| C) | | Type of Erosion | | |
| | | Observations | | |
| | | Incision | Lateral Migration | Precision |
| Predictions | Incision | 39 | 5 | 89% |
| | Lateral Migration | 7 | 161 | 96% |
| | S/R/A | S = 85% | R = 97% | A = 94% |

| | |
|---|---|
| F1 Score | 95.4% |
| Kappa | 83.1% |
| AUC | 94% |
| Over-fitting | 0.8% |

**5.4.3) Distribution of confidence levels and predictions**

Figure 5.4 compares the distribution of confidence levels for the manually classified reference points where it accurately predicted the fluvial hazards (green) with the confidence levels for the points where it did not accurately predict hazards (red). The distributions for the accurately predicted points are concentrated in the medium and high confidence classes with 93.2%, 86.0%, and 96.8% of the points falling within these categories for the PFM, PMM, and TEM models, respectively. Of these accurately predicted points, 51.0%, 43.3%, and 77.5% were in the high confidence class for the PFM, PMM, and TEM models, respectively. While for the incorrectly predicted points 33.9%, 52.9%, and 61.5% of the points were in the uncertain class for the PFM, PMM, and TEM models, respectively and 89.7%, 98.7%, and 94.2% were below the threshold for the high confidence class. This indicates that when the model is correct in its prediction, it is likely to have a higher level of confidence, whereas when the model is incorrect, this will generally result in lower levels of confidence. The confidence level of the prediction is therefore a good metric to examine when making decisions based on the results of these models. It is also useful that the PFM and PMM models present a wide range of confidence levels, as these hazards are not binary (presence/absence) as the models show, but the areas that will be flooded or eroded vary over time depending on factors such as meteorological conditions and river discharge. These are factors that are not taken into account in these models, but the wide range of confidence levels can be used as a proxy for the probability of hazards occurrence based on these factors. For example the flooding model is trained to recognize areas that will be flooded during a 20-year flood. The points with high confidence levels will therefore be flooded during a 20-year flood or perhaps even during smaller floods. On the other hand, points with lower confidence levels that still predict the presence of flooding may require larger than 20-year recurrence floods to be inundated, which doesn't mean that they are safe from flooding.

*Figure 5.4: Distribution of confidence levels for the reference points where it accurately predicted the fluvial hazards (green) and the confidence levels for the points where it did not accurately predict the hazards (red) for A) flooding (PFM), B), mobility (PMM) and C) type of erosion (TEM).*

## 5.4.4) Importance of each variable

Figure 5.5 presents the variable importance test for the three models. For the flood model, the two confinement variables (LocConfRatio and RelConfRatio) are quite important in determining whether flooding will occur, which is to be expected as the more confined the river, the less likely it is that flooding will occur. Other variables that are important in differentiating flood-prone from non-flood-prone areas are location within the catchment (drainage area and mean upstream slope (Mean_slope)). The usefulness of binary variables is not reflected in this type of analysis relative to continuous variables, however we can see that the level of vegetation, the presence of farmland and wetlands are also important variables for determining flood-prone areas. Although USP was not the most important variable when constructing the trees (reflected in its low MDI) it did prove to be one of the most important variables to properly calculate. Indeed, randomizing this variable had a large impact on the accuracy of the model (reflected in

37

its relatively high MDA). As far as mobility is concerned, upstream conditions were very useful in predicting whether a point would be mobile or not, the three most important variables being upstream slope, drainage area, and drainage ratio. These variables will impact both the type and quantity of sediments reaching the reference points but also the velocity of the water. Higher values result in faster flow and larger quantities and sizes of sediments, as they represent more abrupt slopes upstream and less waterbodies such as lakes that can slow down the flow of water and trap sediments. The other variable that was useful for determining if a point will be mobile is the local sinuosity (mean angle of deviation) which allows the models to differentiate between the apex of meanders, which tend to be more mobile, and the more linear segments, which tend to be less mobile. During model training to differentiate between lateral migration and incision, the variables all have roughly identical levels of importance. Only sinuosity of the homogeneous reach shows significantly higher levels of importance, followed by USP and local sinuosity. It makes sense that the model is using the sinuosity to differentiate between incision and lateral migration as lateral migration is the main process that creates sinuous rivers. Consequently, a sinuous river is likely to exhibit lateral migration rather than incision. However, this is not always the case, such as in streams where a geologic confinement forces the river to be sinuous regardless of erosional processes, which is why it is important that the model considers more than just the sinuosity of the river.
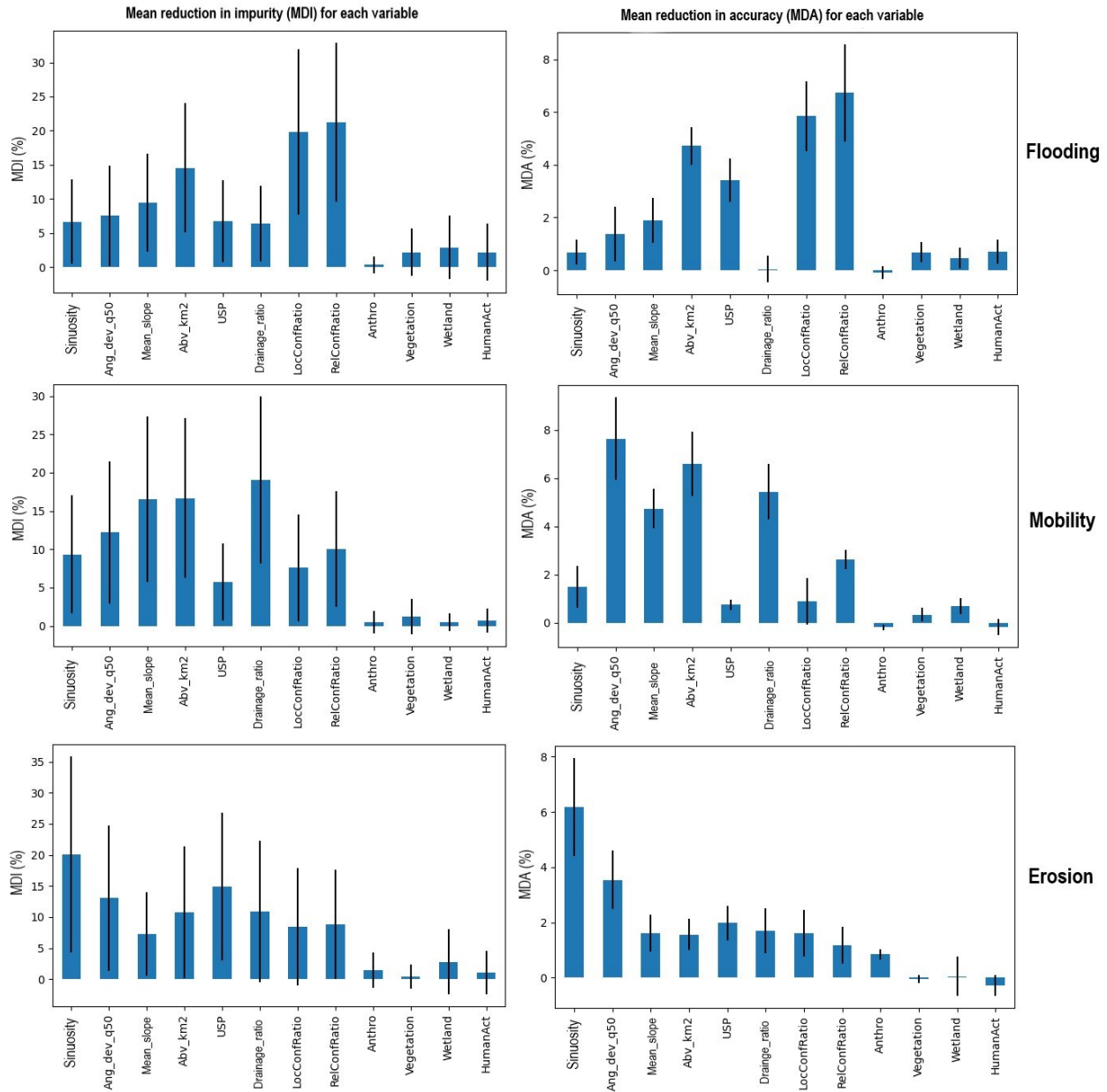
*Figure 5.5: Importance of each variable for the three models using the mean reduction of impurity and mean reduction of accuracy metrics. Variables include the mean angle of deviation between reference points (Ang_dev_q50), local and relative confinement ratios (LocConfRatio and RelConfRatio), presence of bank occupations (Towns/roads = Anthro, farms = HumanAct, vegetation and wetlands) and other hydro geomorphic variables.*

## 5.5) Discussion

Fluvial hazards can have devasting effects on local populations by flooding their homes and vital infrastructure or by damaging crucial road infrastructure that allows emergency services access to access the community or community members to travel to and from their home. Therefore, predicting which road infrastructure is potentially at risk of being damaged is crucial to avoid communities becoming isolated and to continue having access to emergency services and food deliveries. The problem in determining which road infrastructures are potentially at risk is the size of both the river and road networks as well as the number of variables to be taken into

39

account. ML models are increasingly being used to solve this problem, as they can be applied to large areas while taking many variables into account (Ho & Goethals, 2022). While many ML models have been developed to detect areas that are at risk of flooding, we were unable to find any that were trained to detect river mobility. The flood models are also rarely focused on hydro-geomorphological variables and focus on punctual variables rather than variables quantifying the type of river (ex: sinuosity and confinement) or the upstream conditions (ex: mean upstream slope) that can have a large impact on the flood or mobility risk (Figure 5.5) (Wang et al., 2015; Ghosh & Dey, 2021; Hasan et al., 2023; Razavi-Termeh et al., 2023; Youssef et al., 2023).

Not considering these variables is problematic when attempting to quantify the risk of flooding caused by rivers or whether those rivers will be mobile. As highlighted in Figure 5.5, the most important variables for the three models in this study differed based on the model but overall included variables that are seldom considered in ML models for natural hazards, namely confinement level, upstream conditions (mean slope and drainage ratio) and sinuosity of the river. When hydro-geomorphological variables have been included in ML models for flooding, they have been found to be some of the most important variables (Fang et al., 2022). This highlights the wide range of variables and factors that need to be taken into account when assessing river hazards and which require a specific expertise to be properly evaluated. It shows how ML models such as those presented in this study can be used to provide a easy-to-interpret assessment of these variables for experts who do not have the necessary skills.

It is clearly important that methods are developed for the precise extraction of hydro-geomorphological variables at large scale and that important data sources such as high-resolution LiDAR are collected and made available to researchers. The availability of a large-scale public database containing hydro-geomorphological variables for the province's rivers was crucial in this study and facilitated the implementation of ML models to predict which areas of the province were most at risk of being impacted by fluvial hazards. It is recommended that similar databases be developed and maintained for other regions in order to facilitate and encourage further studies at developing tools and methods to better protect communities from the deleterious consequences of fluvial hazards. The results of models such as those presented in this study could also be included in these databases in order to provide stakeholders, whose expertise and level of education vary, with an easy-to-interpret measure of whether or not their community is at risk. Making information such as the potential occurrence of fluvial hazards available to the public would also help to empower smaller-scale stakeholders, such as individuals or local organizations, who have a vested interest in protecting their communities from fluvial hazards, but who rarely receive the information they need to participate in informed discussions on the subject.

### 5.5.1) Use of the results

The main objective of the three RF models is to identify road infrastructure that may be affected by fluvial hazards. In section 5.4.2 the results show how we can use the models to evaluate which watershed has the most hazardous rivers, although that does not inform decision makers about which watershed has the most at-risk infrastructure/communities. By using a simple proximity analysis quantifying the average hazard confidence level predicted in a 200-meter radius around provincially managed bridges, the exposure of this type of road infrastructures can be determined using the RF models. Figure 5.6 presents the results of this buffer analysis for the PFM and PMM models. In the Cascapédia River, there are not many provincially managed

bridges in this watershed due to the local topography that restricts road building in narrow river valleys. As a result, bridges are mainly located at confluences between the major rivers and highly confined, steep slope tributaries, which are highly dynamic areas. This is reflected in the model results where the bridges in the Cascapédia were predicted as being in potentially highly hazardous areas. The Du Gouffre and Nicolet watersheds have less topographical constraints for road construction, with bridges being built in a diversity of conditions. Similar proximity analyses can be used to evaluate other structures such as roads, individual buildings, or communities.

Risk is defined in the World Risk Report as a function of the community's exposure to natural hazards and the community's vulnerability to hazards (De Almeida et al., 2016; Atwii et al., 2022). The vulnerability is the community's ability to resist being damaged from the exposure or recover from the damages the exposure caused. This vulnerability is quantified using variables such as the average age, salary, and educational backgrounds of the community members or number of access routes permitting emergency services to reach the area (Fekete, 2009; Chen et al., 2013; De Almeida et al., 2016) The results of the models in this study can be used to measure the exposure of communities or structures (Figure 5.6) to natural fluvial hazards at the local scale but also at larger scales using aggregation methods (municipal, regional, watershed, etc.). Combining the results from both tools can provide information to decision makers not only about which structures/communities will potentially be exposed to natural hazards, but also about the potential socio-economic impacts if vital road structures were left unusable by fluvial processes or the community was inundated by a flood. This combination can provide a rapid large-scale preliminary assessment of where attention should be concentrated to reduce the potential for communities to be negatively impacted by fluvial processes.
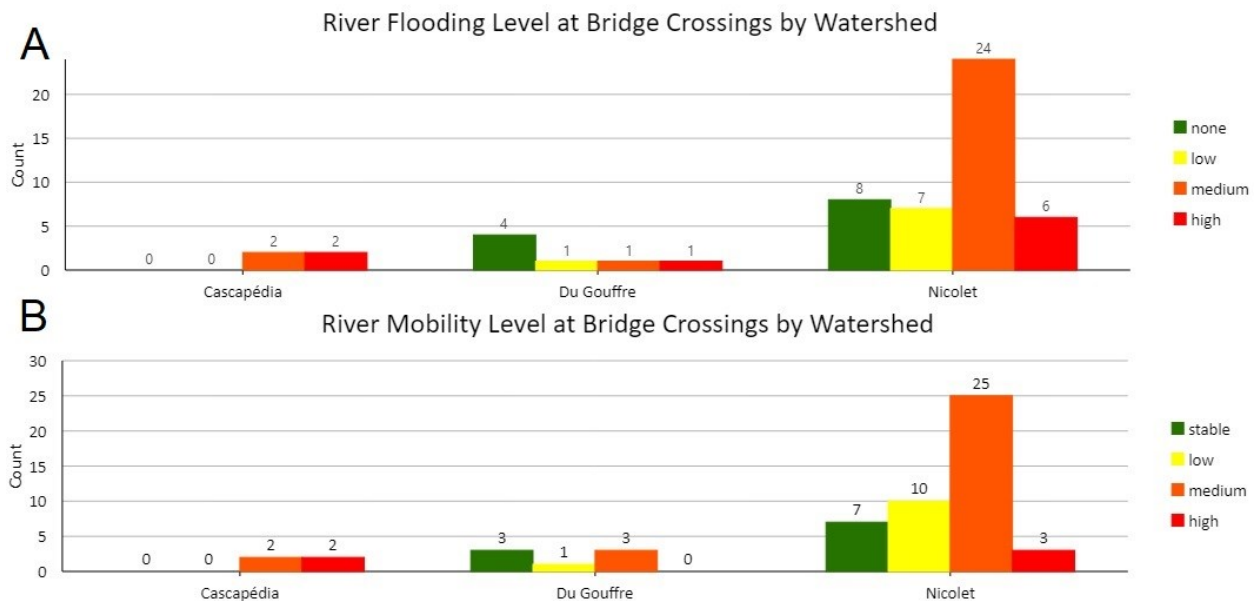


*Figure 5.6: Average fluvial hazard level in a 200-meter radius around bridges managed by the provincial government for A) flooding and B) mobility. < 50% confidence = none/stable, 50 - 55% = low, 56 – 75% = medium, >= 76 % = high.*

Clustering methods can help to visually analyse the potential for infrastructure or communities to be impacted by these fluvial hazards. Figure 5.7 shows a heat map generated for the Du Gouffre watershed with only the points predicted as mobile by the PMM, using the confidence level as a weighting factor. Overlaying the river and road networks over these heat maps reveals the potentially vulnerable road network segments (identified with red circles). A flood event that took place in early May 2023, after the model was completed, revealed that many of these areas were indeed seriously affected by river mobility (photos in Figure 5.7). This method can be used to identify the most at-risk infrastructure at a coarse scale.
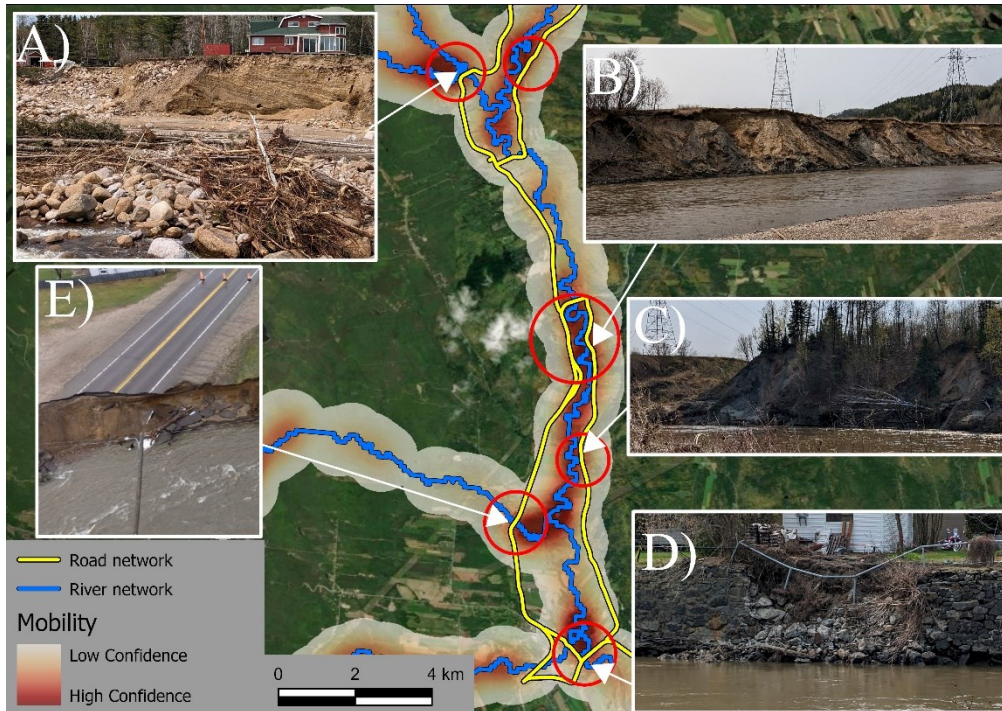


*Figure 5.7: Heat map of the presence of mobility model results weighted by the confidence level with photos of erosion in these areas following a large flood that occurred in May 2023. Photo credit: MELCCFP (A, B, C, and D) & THE CANADIAN PRESS/Jacques Boissinot (E)*

Once individual at-risk infrastructures are identified, a more fine-scale analysis can be carried out by analyzing the predictions and confidence levels for individual reference points. Figure 5.8 shows the results from a bridge crossing one of the confluences between the high-energy tributaries of the Cascapédia and the Cascapédia River itself, as well as photos of when this bridge was damaged by fluvial processes. The labels for the reference points correspond to the confidence levels from the PPM that the area will be mobile or stable. The colour of the points represents the results of the TEM to display the type of erosion predicted and the model's confidence in that prediction, with darker colours representing a higher level of confidence.

The PMM predicted with high confidence that this tributary of the Cascapédia River is mobile with the confidence levels for the reference points ranging from 81% to 93% for presence of mobility (Figure 5.8A/B). The TEM results indicate with high confidence that the mobility in the confined portion of the tributary will be incision before transitioning to medium confidence of lateral migration near the confluence (Figure 5.8A/B). The bridge close to the confluence was

42

damaged by fluvial processes in 2020 (Figure 5.8C) and then repaired (Figure 5.8D) which helps validate that this area is indeed mobile. In Figure 5.8D the bank shows signs of lateral migration just upstream of the bridge, with a point bar forming and exposed banks. The quantity and size of sediment deposited on the bar and under the bridge also show signs of significant upstream sediment transport, which could indicate that incision is occurring upstream.
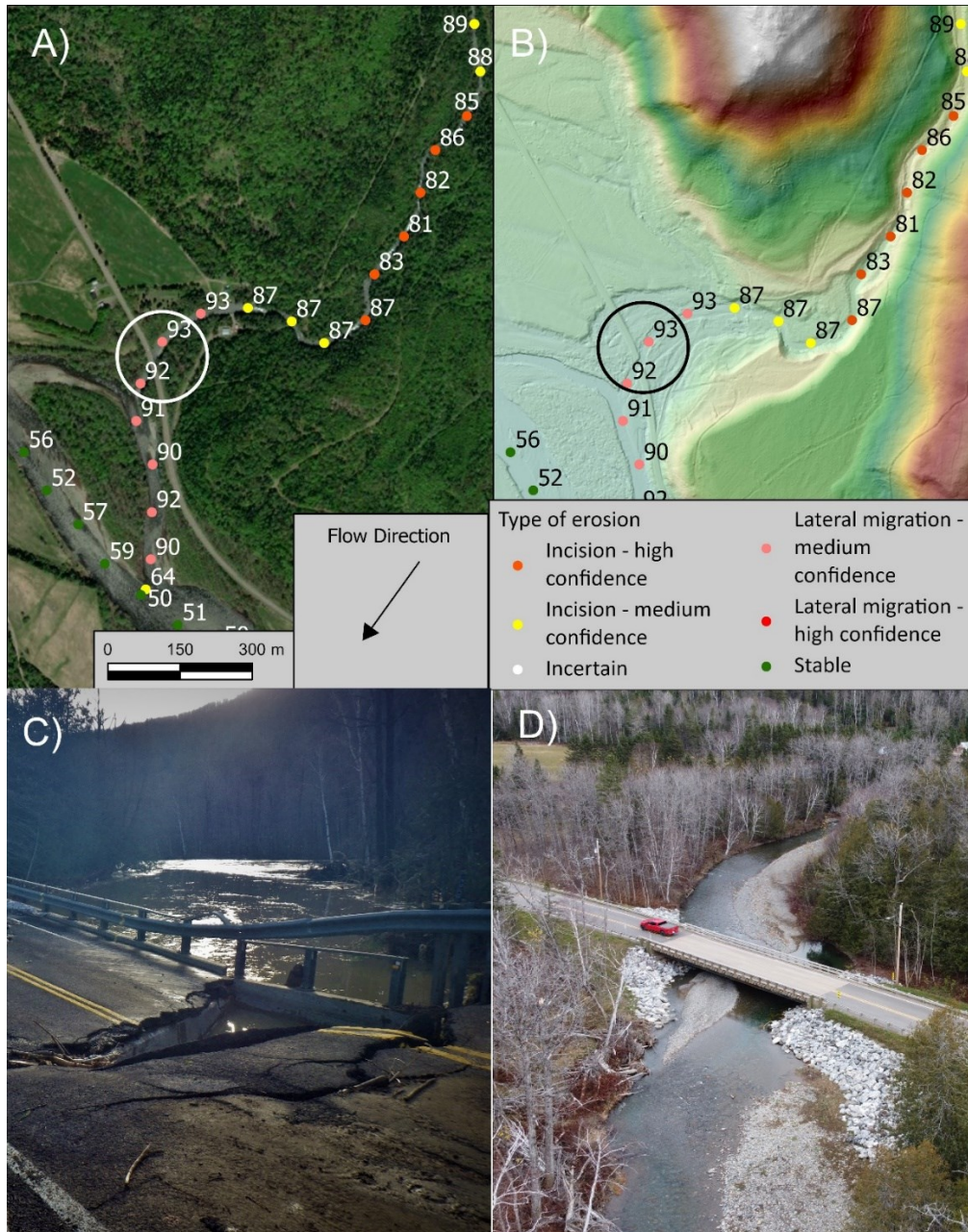


*Figure 5.8: A) and B) Maps illustrating the results of two separate models: presence of mobility and type of erosion model for a mobile tributary of the Cascapédia river (A & B). The labels represent the presence of mobility confidence level. C) photograph of the bridge circled in A and B when it was damaged in 2020. Photo credit: Quebec's Ministry of Transportation D) photograph of the bridge in 2022. Photo credit: Alex Delisle Thibeault.*

This highlights how the model results can be used at multiple scales to conduct a rapid top-down analysis of fluvial hazards over a large territory. This involves firstly identifying which

43

watersheds of the territory should be prioritized, then identifying where within the watershed areas that should be given priority, then determining where the hazardous areas are within these watersheds and what the specific structures at risk are, and then carrying out a spot analysis to determine the specific hazards and conditions that influence the level of risk.

### 5.5.2) Limitations

ML models do come with limitations that impacted the results of this study. These models perform better when the training data is well balanced between the desired classes, although natural patterns of fluvial processes are not as well balanced. This balance also varies depending on the watershed's geomorphological conditions and study area. This study was focused on larger rivers rather than headwater streams due to data availability limitations. This led to an imbalance in the training data for the type of erosion, as an abundance of lateral migration training points were collected. However, as incision occurs mainly, but not exclusively, in headwater streams, it was more difficult to collect data on incision in the study area. The impact of this phenomenon can be seen in the better validation indices of the TEM model compared with the other two models.

Data extraction and preparation at large scale often has extraction errors that occur due to the quality of the data and methods. This study encountered multiple data quality issues stemming from the CRHQ and developed tools. The main issue was with the final point of tributaries in a confluence in the CRHQ having values from the main channel rather than the tributary's values. Another problem concerned the homogenous reaches of the Cascapédia River, many of which were not well segmented, with the result that some reaches were only 100 m long and had only one reference point, which poses problems when it comes to referencing sinuosity and relative confinement when training the models. The developed confinement tool has issues of overestimating the valley width in very sinuous unconfined reaches by approximately 10% on average.

### 5.6) Conclusion

ML models were successfully used as preliminary assessment tools to detect the potential occurrence of fluvial hazards along the river networks of three large watersheds in Quebec (Canada). Computational power, processing time, and budget requirements were relatively low compared with other methods, making this type of modelling particularly promising. Sensitivity analysis revealed that it is important to calibrate the parameters of the chosen model to avoid over-training, allowing the models to generalize to other areas they were not trained on. Preliminary tests on un-trained watersheds show the models are capable to accurately predict the location of hazards in areas where it was not trained. It is equally important to balance the number of data points in each class to allow the model to properly determine the patterns that will allow the model to distinguish between them. The models had validation indices comparable to other ML studies that were ranked as being very good to excellent predictor models. The results are usable at various scales to determine the portion of infrastructure at-risk per watershed, identify which areas within it are hazardous, what factors are influencing the hazards and punctual locations which are hazardous. The importance of each predictor variable in predicting fluvial hazard was quantified and varied based on the hazard being predicted with the most influential variables being the confinement of the river, the sinuosity, and sediment transport proxies.

44

# 6) General Conclusion

In this study the RF classifier ML model was applied with a novel approach for natural hazard detection using reference points every 100-m along the river network combined with hydro-geomorphological variables and processes to predict the potential for fluvial hazards to occur. This methodology provides easily interpretable predictions of where flooding and mobility will occur along the river network with confidence levels indicating how hazardous the area is. This method has various advantages compared to other methods of natural hazard detection including low processing power requirements, short run times, flexibility in choice of input variables (increased adaptability to available data), and the consideration of numerous influential variables that provides a holistic analysis of the local conditions rather than relying on a few key variables. Through this analysis it was found that the main factors influencing flooding are the confinement of the river and its location within the watershed. This is an important finding as many ML applications to detect flooding do not include the confinement of the river. For mobility, the most important influential factors were the proxies for sediment transport and the local sinuosity. No other studies were found using ML to directly detect river mobility, however future studies should consider that it will be important to consider these upstream conditions and not concentrate only on local variables. It is also key to consider the local sinuosity and not the more commonly used homogenous reach sinuosity.

The findings from this research are important for infrastructure planning as they indicate that planners should be considering factors upstream of the potential construction sites and not only in the surrounding area. In Quebec, the Ministry of Transportation has until now only included a geomorphological analysis close to their infrastructure (in the range of around 200 m upstream and downstream of a bridge or culvert). The modelling tools developed in this project will go a long way to helping them better anticipate problems that could arise in river sections further upstream. The tools were indeed presented to a team of GIS experts of the MTMD in June 2023, and it is hoped that they will soon be integrated in their GIS system.

Discussions are also under way with the MTMD to ensure that they document fluvial hazards more efficiently in a centralized database. This would provide invaluable training data to improve the RF tools which can then be applied in more watersheds. Future studies should also test if adding more predictor variables such as upstream land cover and climatic data could improve the accuracy of the modelling tools.

# References

1.  Anderson, I., Rizzo, D. M., Huston, D. R., & Dewoolkar, M. M. (2017). Stream Power Application for Bridge-Damage Probability Mapping Based on Empirical Evidence from Tropical Storm Irene. *Journal of Bridge Engineering*, *22*(5), 05017001. https://doi.org/10.1061/(ASCE)BE.1943-5592.0001022

2.  Ashmore, P., McDonald, J., Barlow, V. (2023) Multi-decadal changes in river morphology in an urbanizing watershed: Highland Creek, Toronto, Canada. Geomorphology, 433, 108710, 1-26.

3.  Arabameri, A., & Pourghasemi, H. R. (2019). 13 - Spatial Modeling of Gully Erosion Using Linear and Quadratic Discriminant Analyses in GIS and R. In H. R. Pourghasemi & C. Gokceoglu (Eds.), *Spatial Modeling in GIS and R for Earth and Environmental Sciences* (pp. 299–321). Elsevier. https://doi.org/10.1016/B978-0-12-815226-3.00013-2

4.  Atwii, F., Sandvik, K., & Kirch, L. (2022). WorldRiskReport 2022. Bündnis Entwicklung Hilft Ruhr University Bochum – Institute for International Law of Peace and Armed Conflict (IFHV). https://weltrisikobericht.de/wp-content/uploads/2022/09/WorldRiskReport-2022_Online.pdf

5.  Avila-Aceves, E., Plata-Rocha, W., Monjandin-Armenta, S. A., & Rangel-Peraza, J. G. (2023). Geospatial modelling of floods: a literature review. Stochastic Environmental Research and Risk Assessment. https://doi.org/10.1007/s00477-023-02505-1

6.  Bagnold, R. A. (1966). *An approach to the sediment transport problem from general physics* (No. 422–I). U. S. Govt. Print. Off.,. https://doi.org/10.3133/pp422I

7.  Bangen, S., Kramer, N., Wheaton, J. M., & Bouwes, N. (2017). *The GUTs of the Geomorphic Unit Tool (GUT): What is under the hood*. https://doi.org/10.13140/RG.2.2.31118.66884

8.  Barakat, A., Rafai, M., Mosaid, H., Islam, M. S., & Saeed, S. (2023). Mapping of Water-Induced Soil Erosion Using Machine Learning Models: A Case Study of Oum Er Rbia Basin (Morocco). Earth Systems and Environment, 7(1), 151–170. https://doi.org/10.1007/s41748-022-00317-x

9.  Beechie, T. J., Liermann, M., Pollock, M. M., Baker, S., & Davies, J. (2006). Channel pattern and river-floodplain dynamics in forested mountain river systems. *Geomorphology*, *78*(1–2), 124–141. https://doi.org/10.1016/j.geomorph.2006.01.030

10. Beechie, T., & Imaki, H. (2014). Predicting natural channel patterns based on landscape and geomorphic controls in the Columbia River basin, USA: Predicting Channel Patterns in the Columbia Basin. *Water Resources Research*, *50*(1), 39–57. https://doi.org/10.1002/2013WR013629

11. Benyahya, L., A. Daigle, D. Caissie, D. Beveridge et A. St-Hilaire (2009). Caractérisation du régime naturel du débit des bassins versants de l'Est du Canada. INRS-ETE, rapport R1057, 88 pages.

12. Belletti, B., Rinaldi, M., Bussettini, M., Comiti, F., Gurnell, A. M., Mao, L., Nardi, L., & Vezza, P. (2017). Characterising physical habitats and fluvial hydromorphology: A new

system for the survey and classification of river geomorphic units. *Geomorphology*, *283*, 143–157. https://doi.org/10.1016/j.geomorph.2017.01.032

13. Bernier, J.-F., Chassiot, L., & Lajeunesse, P. (2021). Assessing bank erosion hazards along large rivers in the Anthropocene: a geospatial framework from the St. Lawrence fluvial system. *Geomatics, Natural Hazards and Risk*, *12*(1), 1584–1615. https://doi.org/10.1080/19475705.2021.1935333

14. Breiman, L. (2001). Random Forests. *Machine Learning*, *45*(1), 5–32. https://doi.org/10.1023/A:1010933404324

15. Brierley, G. J., & Fryirs, K. A. (Eds.). (2004). *Geomorphology and River Management*. Blackwell Publishing. https://doi.org/10.1002/9780470751367

16. Biron, P. M., Choné, G., Buffin-Bélanger, T., Demers, S., & Olsen, T. (2013). Improvement of streams hydro-geomorphological assessment using LiDAR DEMs: STREAMS HYDRO-GEOMORPHOLOGICAL ASSESSMENT USING LiDAR DEMs. Earth Surface Processes and Landforms, 38(15), 1808–1821. https://doi.org/10.1002/esp.3425

17. Biron, P. M., Buffin-Bélanger, T., Larocque, M., Choné, G., Cloutier, C.-A., Ouellet, M.-A., Demers, S., Olsen, T., Desjarlais, C., & Eyquem, J. (2014). Freedom Space for Rivers: A Sustainable Management Approach to Enhance River Resilience. *Environmental Management*, *54*(5), 1056–1073. https://doi.org/10.1007/s00267-014-0366-z

18. Bizzi, S., & Lerner, D. N. (2015). The Use of Stream Power as an Indicator of Channel Sensitivity to Erosion and Deposition Processes: SP AS AN INDICATOR OF EROSION AND DEPOSITION. *River Research and Applications*, *31*(1), 16–27. https://doi.org/10.1002/rra.2717

19. Bowman, H., Jeffries, R., Ing, R., Hemsworth, M., Todd-Burley, N., Hankin, B., Soar, P., & Thorne, C. (2021). Investigating ways to predict channel changes to inform flood risk management now and in the future. Science and Practice for an Uncertain Future, null-null. https://doi.org/10.3311/FloodRisk2020.2.26

20. Borselli, L., Cassi, P., & Torri, D. (2008). Prolegomena to sediment and flow connectivity in the landscape: A GIS and field numerical assessment. *CATENA*, *75*(3), 268–277. https://doi.org/10.1016/j.catena.2008.07.006

21. Brooks, G., & Lawrence, D. (2000). Geomorphic Effects of Flooding Along Reaches of Selected Rivers in the Saguenay Region, Québec, July 1996. *Géographie Physique et Quaternaire*, *54*(3), 281–299. https://doi.org/10.7202/005639ar

22. Buffin-Bélanger T., Demers S. et Olsen T. (2015) – Diagnostic hydrogéomorphologique pour mieux considérer les dynamiques hydrosédimentaires aux droits des traverses de cours d'eau : guide méthodologique. Laboratoire de géomorphologie et de dynamique fluviale, Université du Québec à Rimouski. Remis au ministère des Transports du Québec, Mars 2015, 55 pages.

23. Buitinck, L., Louppe, G., Blondel, M., Pedregosa, F., Mueller, A., Grisel, O., Niculae, V., Prettenhofer, P., Gramfort, A., Grobler, J., Layton, R., Vanderplas, J., Joly, A., Holt, B.,

& Varoquaux, G. (2013). API design for machine learning software: experiences from the scikit-learn project. https://doi.org/10.48550/ARXIV.1309.0238

24. Buraas, E. M., Renshaw, C. E., Magilligan, F. J., & Dade, W. B. (2014). Impact of reach geometry on stream channel sensitivity to extreme floods. *Earth Surface Processes and Landforms*, *39*(13), 1778–1789. https://doi.org/10.1002/esp.3562

25. Bywater-Reyes, S., Diehl, R. M., Wilcox, A. C., Stella, J. C., & Kui, L. (2022). A Green New Balance: Interactions among riparian vegetation plant traits and morphodynamics in alluvial rivers. *Earth Surface Processes and Landforms*, esp.5385. https://doi.org/10.1002/esp.5385

26. Cammeraat, L. H. (2002). A review of two strongly contrasting geomorphological systems within the context of scale. *Earth Surface Processes and Landforms*, *27*(11), 1201–1222. https://doi.org/10.1002/esp.421

27. Cavalli, M., Crema, S., Trevisani, S., & Marchi, L. (2017). GIS tools for preliminary debris-flow assessment at regional scale. *Journal of Mountain Science*, *14*(12), 2498–2510. https://doi.org/10.1007/s11629-017-4573-y

28. CEHQ. (2021). CEHQ ZIS. Retrieved December 30, 2021, from https://www.cehq.gouv.qc.ca/zones-inond/ZIS-20190715/index.html

29. Chen, W., Cutter, S. L., Emrich, C. T., & Shi, P. (2013). Measuring social vulnerability to natural hazards in the Yangtze River Delta region, China. International Journal of Disaster Risk Science, 4(4), 169–181. https://doi.org/10.1007/s13753-013-0018-6

30. Choné, G. and Biron, P.M. (2016) Assessing the relationship between river mobility and habitat. River Research and Applications, 32, 528-539

31. Choné, G., Biron, P. M., Buffin-Bélanger, T., Mazgareanu, I., Neal, J. C., & Sampson, C. C. (2021). An assessment of large-scale flood modelling based on LiDAR data. Hydrological Processes, 35(8). https://doi.org/10.1002/hyp.14333

32. Choné, G., Mazgareanu, I., Gauthier-Dufour, E., Biron, P., Buffin-Bélanger, T. (2022) Vers une cartographie générale des zones inondables : Phase 2.2 – Modélisation hydraulique appliquée à large échelle pour des cours d'eau du Québec habité. Rapport final, Ministère de l'Environnement et de la Lutte contre les changements climatiques, March 2022, 267 p

33. Church M. (1992). Channel morphology and typology. In The Rivers Handbook, ed. P Calow, GE Petts, 1:126–43. Oxford: Blackwell Sci. 526 pp.

34. Church, M. (2006). BED MATERIAL TRANSPORT AND THE MORPHOLOGY OF ALLUVIAL RIVER CHANNELS. *Annual Review of Earth and Planetary Sciences*, *34*(1), 325–354. https://doi.org/10.1146/annurev.earth.33.092203.122721

35. Concordia River Management Lab. (2021). *ConcordiaRiverTools*. GitHub. https://github.com/gchone/ConcordiaRiverLab-RiversTools

36. Costabile, P., Macchione, F., Natale, L., & Petaccia, G. (2015). Flood mapping using LIDAR DEM. Limitations of the 1-D modeling highlighted by the 2-D approach. Natural Hazards, 77(1), 181–204. https://doi.org/10.1007/s11069-015-1606-0

37. Crema, S., & Cavalli, M. (2018). SedInConnect: A stand-alone, free and open-source tool for the assessment of sediment connectivity. *Computers & Geosciences*, *111*, 39–45. https://doi.org/10.1016/j.cageo.2017.10.009

38. De Almeida, L. Q., Welle, T., & Birkmann, J. (2016). Disaster risk indicators in Brazil: A proposal based on the world risk index. International Journal of Disaster Risk Reduction, 17, 251–272. https://doi.org/10.1016/j.ijdrr.2016.04.007

39. Demers S., Olsen T. et Buffin-Bélanger T. 2014. Développement d'une méthode hydrogéomorphologique pour mieux considérer les dynamiques hydrosédimentaires aux droits des traverses de cours d'eau du Bas-Saint-Laurent et de la Gaspésie dans le contexte de changements climatiques et environnementaux. Laboratoire de géomorphologie et de dynamique fluviale, Université du Québec à Rimouski. Remis au ministère des Transports du Québec, décembre 2014. 202 p

40. Direction de l'expertise hydrique. (2018). Document d'accompagnement de l'Atlas hydroclimatique du Québec méridional. Québec, ministère du Développement durable, de l'Environnement et de la Lutte contre les changements climatiques, 34 p.

41. Dunne T, Leopold LB. 1978. Water in Environmental Planning. WH Freeman: San Francisco.

42. Fairbridge, R. W. (2006). The Earth Sciences Enclopedia Online (ESEO): Geomorphology. Springer Berlin / Heidelberg.

43. Fekete, A. (2009). Validation of a social vulnerability index in context to river-floods in Germany. Natural Hazards and Earth System Sciences, 9(2), 393–403. https://doi.org/10.5194/nhess-9-393-2009

44. Fontana, G. D., & Marchi, L. (2002). Slope-area relationships and sediment dynamics in two alpine streams. *Hydrological Processes*, *17*(1), 73–87. https://doi.org/10.1002/hyp.1115

45. Florsheim, J., Mount, J., Chin, A. (2008). Bank erosion as a desirable attribute of rivers. Bioscience, 58, 521-529.

46. Fryirs, K. A., & Brierley, G. J. (2013). *Geomorphic analysis of river systems: an approach to reading the landscape*. Wiley-Blackwell.

47. Fryirs, K. A., & Brierley, G. J. (2018). What's in a name? A naming convention for geomorphic river types using the River Styles Framework. *PLOS ONE*, *13*(9), e0201909. https://doi.org/10.1371/journal.pone.0201909

48. Fryirs, K., & Brierley, G. (2022). Assemblages of geomorphic units: A building block approach to analysis and interpretation of river character, behaviour, condition and recovery. *Earth Surface Processes and Landforms*, *47*(1), 92–108. https://doi.org/10.1002/esp.5264

49. Gartner, J. D., Dade, W. B., Renshaw, C. E., Magilligan, F. J., & Buraas, E. M. (2015). Gradients in stream power influence lateral and downstream sediment flux in floods. *Geology*, *43*(11), 983–986. https://doi.org/10.1130/G36969.1

50. Gartner, J. (2016). Stream Power: Origins, Geomorphic Applications, and GIS Procedures. *Water Publications*. https://scholarworks.umass.edu/water_publications/1

51. *Geomorphic Unit Quick Reference Guide*. (2022). River Styles. https://riverstyles.com/river-styles-toolkit/geomorphic-unit-quick-reference-guide/

52. Ghosh, A., & Dey, P. (2021). Flood severity assessment of the coastal tract situated between Muriganga and Saptamukhi estuaries of Sundarban delta of India using Frequency Ratio (FR), Fuzzy Logic (FL), Logistic Regression (LR) and Random Forest (RF) models. Regional Studies in Marine Science, 42, 101624. https://doi.org/10.1016/j.rsma.2021.101624

53. Gombault, C., Bossé, C., Lapointe, M. et Blais-Gagnon, A., C., (2022). Guide d'utilisation des données géospatiales de la couverture pédologique du Québec. IRDA. 68 pages. © Institut de recherche et de développement en agroenvironnement inc. (IRDA)

54. Gonzales-Inca, C., Calle, M., Croghan, D., Torabi Haghighi, A., Marttila, H., Silander, J., & Alho, P. (2022). Geospatial Artificial Intelligence (GeoAI) in the Integrated Hydrological and Fluvial Systems Modeling: Review of Current Applications and Trends. Water, 14(14), 2211. https://doi.org/10.3390/w14142211

55. González, M. B., Rodríguez-Oroz, D., Alcalá-Reygosa, J., & Campos, N. (2020). Geomorphological mapping and landforms characterization of a high valley environment in the Chilean Andes. Journal of South American Earth Sciences, 104, 102918. https://doi.org/10.1016/j.jsames.2020.102918

56. Gouvernement du Québec. (2021). *Règlement sur l'encadrement d'activités en fonction de leur impact sur l'environnement - chapitre Q-2, r. 17.1*. https://www.legisquebec.gouv.qc.ca/fr/document/rc/Q-2,%20r.%2017.1

57. Gouvernement du Québec. (2022). *Gestion des rives, du littoral et des zones inondables*. https://www.quebec.ca/gouvernement/politiques-orientations/plan-de-protection-du-territoire-face-aux-inondations/gestion-rives-littoral-zones-inondables

58. Greenfield, J., Lahlou, M., Swift, L., Jr., & Manguerra, H.B. (2001). Watershed Erosion and Sediment Load Estimation Tool. *Soil Erosion*. Soil Erosion. https://doi.org/10.13031/2013.3266

59. Guillon, H., Byrne, C. F., Lane, B. A., Sandoval Solis, S., & Pasternack, G. B. (2020). Machine Learning Predicts Reach-Scale Channel Types From Coarse-Scale Geospatial Data in a Large River Basin. Water Resources Research, 56(3). https://doi.org/10.1029/2019WR026691

60. Helm, C., Hassan, M. A., & Reid, D. (2020). Characterization of morphological units in a small, forested stream using close-range remotely piloted aircraft imagery. Earth Surface Dynamics, 8(4), 913–929. https://doi.org/10.5194/esurf-8-913-2020

61. Ho, L., & Goethals, P. (2022). Machine learning applications in river research: Trends, opportunities and challenges. Methods in Ecology and Evolution, 13(11), 2603–2621. https://doi.org/10.1111/2041-210X.13992

62. Ielpi, A., Lapôtre, M. G. A., Gibling, M. R., & Boyce, C. K. (2022). The impact of vegetation on meandering rivers. Nature Reviews Earth & Environment, 3(3), 165–178. https://doi.org/10.1038/s43017-021-00249-6

63. IPCC, 2021: Climate Change 2021: The Physical Science Basis. Contribution of Working Group I to the Sixth Assessment Report of the Intergovernmental Panel on Climate Change [Masson-Delmotte, V., P. Zhai, A. Pirani, S.L. Connors, C. Péan, S. Berger, N. Caud, Y. Chen, L. Goldfarb, M.I. Gomis, M. Huang, K. Leitzell, E. Lonnoy, J.B.R. Matthews, T.K. Maycock, T. Waterfield, O. Yelekçi, R. Yu, and B. Zhou (eds.)]. Cambridge University Press. In Press.

64. Jautzy, T., Herrault, P.-A., Chardon, V., Schmitt, L., & Rixhon, G. (2020). Measuring river planform changes from remotely sensed data – a Monte Carlo approach to assessing the impact of spatially variable error. Earth Surface Dynamics, 8(2), 471–484. https://doi.org/10.5194/esurf-8-471-2020

65. Jia, G. W., Zhan, T. L. T., Chen, Y. M., & Fredlund, D. G. (2009). Performance of a large-scale slope model subjected to rising and lowering water levels. *Engineering Geology*, *106*(1-2), 92–103. https://doi.org/10.1016/j.enggeo.2009.03.003

66. Johansen, K., Tiede, D., Blaschke, T., Arroyo, L. A., & Phinn, S. (2011). Automatic Geographic Object Based Mapping of Streambed and Riparian Zone Extent from LiDAR Data in a Temperate Rural Urban Environment, Australia. *Remote Sensing*, *3*(6), 1139–1156. https://doi.org/10.3390/rs3061139

67. Johnson, M. F., Thorne, C. R., Castro, J. M., Kondolf, G. M., Mazzacano, C. S., Rood, S. B., & Westbrook, C. (2020). Biomic river restoration: A new focus for river management. *River Research and Applications*, *36*(1), 3–12. https://doi.org/10.1002/rra.3529

68. Kasprak, A., Hough-Snee, N., Beechie, T., Bouwes, N., Brierley, G., Camp, R., Fryirs, K., Imaki, H., Jensen, M., O'Brien, G., Rosgen, D., & Wheaton, J. (2016). The Blurred Line between Form and Process: A Comparison of Stream Channel Classification Frameworks. PLOS ONE, 11(3), e0150293. https://doi.org/10.1371/journal.pone.0150293

69. Kavzoglu, T., & Teke, A. (2022). Predictive Performances of Ensemble Machine Learning Algorithms in Landslide Susceptibility Mapping Using Random Forest, Extreme Gradient Boosting (XGBoost) and Natural Gradient Boosting (NGBoost). Arabian Journal for Science and Engineering, 47(6), 7367–7385. https://doi.org/10.1007/s13369-022-06560-8

70. Lauer, J. W. (2006). Channel Planform Statistics Toolbox. National Center for Earth-surface Dynamics. Minneapolis, MN 55414.

71. Leopold, L.B. (1962) Rivers. American Scientist, 50, 4, 511-537; Hack, J.T. 1975. Dynamic Equilibrium and Landscape Evolution, In Melhorn, W.N. and Flemal, R.C. (eds.) Theories of Landform Development, Proceedings of the Sixth Annual Binghampton Symposium, 87-102

72. Lisenby, P. E., Fryirs, K. A., & Thompson, C. J. (2020). River sensitivity and sediment connectivity as tools for assessing future geomorphic channel behavior. *International Journal of River Basin Management*, *18*(3), 279–293. https://doi.org/10.1080/15715124.2019.1672705

73. Li, W., Song, M., Zhou, B., Cao, K., & Gao, S. (2015). Performance improvement techniques for Geospatial Web Services in a cyberinfrastructure environment – a case study with a disaster management portal. *Computers, Environment and Urban Systems*, *54*, 314–325. https://doi.org/10.1016/j.compenvurbsys.2015.04.003

74. Li, X., & Wei, X. (2014). Analysis of the relationship between soil erosion risk and surplus floodwater during flood season. *Journal of Hydrologic Engineering*, *19*(7), 1294–1311. https://doi.org/10.1061/(asce)he.1943-5584.0000912

75. Li, Z., & Fang, H. (2016). Impacts of climate change on water erosion: A Review. *Earth-Science Reviews*, *163*, 94–117. https://doi.org/10.1016/j.earscirev.2016.10.004

76. Louppe, G. (2014). Understanding Random Forests: From Theory to Practice. https://doi.org/10.48550/ARXIV.1407.7502

77. Marchand, J.-P., Buffin-Bélanger, T., Hétu, B., & St-Onge, G. (2014). Stratigraphy and infill history of the glacially eroded Matane River Valley, eastern Quebec, Canada. Canadian Journal of Earth Sciences, 51(2), 105–124. https://doi.org/10.1139/cjes-2013-0054

78. Marchi, L., & Dalla Fontana, G. (2005). GIS morphometric indicators for the analysis of sediment dynamics in mountain basins. *Environmental Geology*, *48*(2), 218–228. https://doi.org/10.1007/s00254-005-1292-4

79. Massé, S., & Buffin-Bélanger, T. (2016). Understanding hydrogeomorphological dynamics and the distribution of large wood jams to promote sustainable river management strategies. *The Canadian Geographer / Le Géographe Canadien*, *60*(4), 505–518. https://doi.org/10.1111/cag.12283

80. Mayer, A., Winkler, R., & Fry, L. (2014). Classification of watersheds into integrated social and biophysical indicators with clustering analysis. Ecological Indicators, 45, 340–349. https://doi.org/10.1016/j.ecolind.2014.04.030

81. Mazgareanu, I., Biron, P. M., & Buffin-Bélanger, T. (2020). A fuzzy GIS model to determine confluence morphological sensitivity to tributary inputs at the watershed scale. *Geomorphology*, *357*, 107095. https://doi.org/10.1016/j.geomorph.2020.107095

82. Miller, A. J. (1990). "Flood hydrology and geomorphic effectiveness in the central Appalachians." Earth Surf. Processes Landforms, 15(2), 119–134.

83. Ministère du Développement durable, de l'Environnement et de la Lutte contre les changements climatiques du Québec (MELCC). (2015). *Guide d'interprétation, Politique de protection des rives, du littoral et des plaines inondables*. Ministère du Développement durable, de l'Environnement et de la Lutte contre les changements climatiques du Québec, Direction des politiques de l'eau. https://www.environnement.gouv.qc.ca/eau/rives/guide-interpretationPPRLPI.pdf

84. Ministère du Développement durable, Ministère de l'Environnement et de la Lutte contre les changements climatiques (MELCC). (2018). Cartographie de l'utilisation du territoire du Québec. Données de SIG [ArcMap, ESRI Canada]. Ministère de l'Environnement et de la Lutte contre les changements climatiques, Gouvernement du Québec, Québec.

85. Ministère du Développement durable, Ministère de l'Environnement et de la Lutte contre les changements climatiques (MELCC). (2021). Cadre de référence hydrologique du Québec : guide de l'utilisateur – version 1.1. 25 p.

86. Ministère du Développement durable, Ministère de l'Environnementet de la Lutte contre les changements climatiques (MELCC). (2022). *Répertoire des barrages*. CEHQ. https://www.cehq.gouv.qc.ca/barrages/default.asp

87. Ministère des Forêts, de la Faune et des Parcs. (2022). foret ouverte. Retrieved January 4, 2022, from https://www.foretouverte.gouv.qc.ca/

88. Ministère des transports. (2019). *Manuel d'inspection des ponceaux*. Bibliothèque et Archives nationales du Québec. http://collections.banq.qc.ca/ark:/52327/3692801

89. Montgomery, D. R., & Buffington, J. M. (1997). Channel-reach morphology in mountain drainage basins. *Geological Society of America Bulletin*, *109*(5), 596–611. https://doi.org/10.1130/0016-7606(1997)109<0596:CRMIMD>2.3.CO;2

90. Mosavi, A., Sajedi-Hosseini, F., Choubin, B., Taromideh, F., Rahi, G., & Dineva, A. (2020). Susceptibility Mapping of Soil Water Erosion Using Machine Learning Models. Water, 12(7), 1995. https://doi.org/10.3390/w12071995

91. Nasr, A., Kjellström, E., Björnsson, I., Honfi, D., Ivanov, O. L., & Johansson, J. (2019). Bridges in a changing climate: a study of the potential impacts of climate change on bridges and their possible adaptations. Structure and Infrastructure Engineering, 16(4), 738–749. https://doi.org/10.1080/15732479.2019.1670215

92. Natural Resources Canada, & Public Safety Canada. (2018). *Federal Flood Mapping Framework* (No. 112e; p. 112e). https://doi.org/10.4095/308128

93. NSERC. (2021). *Flood Map Viewer*. Flood maps viewer. Retrieved December 30, 2021, from https://www.floodmapviewer.com/maps

94. O'Brien, G. R., Wheaton, J. M., Fryirs, K., Macfarlane, W. W., Brierley, G., Whitehead, K., Gilbert, J., & Volk, C. (2019). Mapping valley bottom confinement at the network scale. *Earth Surface Processes and Landforms*, esp.4615. https://doi.org/10.1002/esp.4615

95. Ouellet Dallaire, C., Lehner, B., Sayre, R., & Thieme, M. (2019). A multidisciplinary framework to derive global river reach classifications at high spatial resolution. *Environmental Research Letters, 14(2), 024003. https://doi.org/10.1088/1748-9326/aad8e9*

96. Ouranos. (2015). Vers l'adaptation. Synthèse des connaissances sur les changements climatiques au Québec. Partie 1 : Évolution climatique au Québec. Édition 2015. Montréal, Québec : Ouranos, 114 p.

97. Ouranos. (2021). Flood Frequency Analysis and Dam Safety in the 21st Century Climate. Report submitted to Climate Change Impacts and Adaptation Division, Natural Resources Canada, 37 p.

98. Papangelakis, E., MacVicar, B., Ashmore, P., Gingerich, D., & Bright, C. (2022). Testing a Watershed-Scale Stream Power Index Tool for Erosion Risk Assessment in an Urban River. *Journal of Sustainable Water in the Built Environment, 8(3), 04022008. https://doi.org/10.1061/JSWBAY.0000989*

99. Parker, C., & Davey, J. (2023). Stream power indices correspond poorly with observations of alluvial river channel adjustment. Earth Surface Processes and Landforms, esp.5550. https://doi.org/10.1002/esp.5550

100. Pealer S. 2012. Lessons from Irene: Building resiliency as we rebuild. Vermont Agency of Natural Resources, Waterbury, Vermont.

101. Pedregosa, F., Varoquaux, G., Gramfort, A., Michel, V., Thirion, B., Grisel, O., Blondel, M., Prettenhofer, P., Weiss, R., Dubourg, V., Vanderplas, J., Passos, A., Cournapeau, D., Brucher, M., Perrot, M., & Duchesnay, É. (2011). Scikit-learn: Machine Learning in Python. *Journal of Machine Learning Research, 12(85), 2825–2830. http://jmlr.org/papers/v12/pedregosa11a.html*

102. Petts, G. E., & Gurnell, A. M. (2005). Dams and geomorphology: Research progress and future directions. *Geomorphology, 71(1), 27–47. https://doi.org/10.1016/j.geomorph.2004.02.015*

103. Piégay, H., Darby, S. E., Mosselman, E., & Surian, N. (2005). A review of techniques available for delimiting the erodible river corridor: a sustainable approach to managing bank erosion. River Research and Applications, 21(7), 773–789. https://doi.org/10.1002/rra.881

104. Poff, NLR (2014) Rivers of the Anthropocene? Frontiers in Ecology and the Environment. Guest Editorial https://doi.org/10.1890/1540-9295-12.8.427

105. Reid, H. E., & Brierley, G. J. (2015). Assessing geomorphic sensitivity in relation to river capacity for adjustment. *Geomorphology*, *251*, 108–121. https://doi.org/10.1016/j.geomorph.2015.09.009

106. Rondot, J. (2000). Charlevoix and Sudbury as gravity-readjusted impact structures. Meteoritics & Planetary Science, 35(4), 707–712. https://doi.org/10.1111/j.1945-5100.2000.tb01454.x

107.     Rosso, et al., 2006. A physically based model for the hydrologic control on shallow landsliding. Water Resources Research 42.

108.     Rousseau, Y. and Biron, P.M. (2009) Geomorphological impacts of channel straightening in an agricultural watershed, Southwestern Québec. The Northeastern Geographer, 1, 91-113.

109.     Roux, C., Alber, A., Bertrand, M., Vaudor, L., & Piégay, H. (2015). "fluvialcorridor": A new arcgis toolbox package for multiscale riverscape exploration. *Geomorphology*, *242*, 29–37. https://doi.org/10.1016/j.geomorph.2014.04.018

110.     Roy, G., & Dion, C. (2014). *Symboles et abréviations de la carte géoscientifique*. Direction générale de géologie Québec. Pages 56 – 58.

111.     Riverscapes Consortium. (n.d.). Retrieved January 12, 2022, from https://riverscapes.xyz/

112.     Ruiz-Villanueva, V., Piégay, H., Gurnell, A. M., Marston, R. A., & Stoffel, M. (2016). Recent advances quantifying the large wood dynamics in river basins: New methods and remaining challenges: Large Wood Dynamics. *Reviews of Geophysics*, *54*(3), 611–652. https://doi.org/10.1002/2015RG000514

113.     Russell, M., Mittelstet, A., & Joeckel, M. (2021). Impact of Bank Stabilization Structures on Upstream and Downstream Bank Mobilization at Cedar River, Nebraska. *American Society of Agricultural and Biological Engineers*, *64*(5), 1555–1567. https://doi.org/10.13031/trans.14551

114.     Saadon, Al,, Abdullah, J, N.S. Muhammad, N.S., J. Ariffin, J., Julien, P.Y. (2021) Predictive models for the estimation of riverbank erosion rates. Catena, 196, 104917, 1-12.

115.     Schumm, S. A. (1963). *A tentative classification of alluvial river channels an examination of similarities and differences among some Great Plains rivers* (No. 477). U.S. Geological Survey. https://doi.org/10.3133/cir477

116.     Scoazec, C., & Buffin-Belanger, T. (2019). (rep.). *Développement d'un indice préliminaire pour l'évaluation des processus sédimentaires appliqué à la gestion des traverses de cours d'eau, en Gaspésie, au Québec* .

117.     Sear, D., Hornby, D., Wheaton, J., & Hill, C. (2021). *Understanding river channel sensitivity to geomorphological changes*. Environment Agency.

118.     Sechu, G. L., Nilsson, B., Iversen, B. V., Greve, M. B., Børgesen, C. D., & Greve, M. H. (2020). *A stepwise GIS approach for the delineation of river valley bottom within drainage basins using a cost distance accumulation analysis* [Preprint]. Rivers and Lakes/Remote Sensing and GIS. https://doi.org/10.5194/hess-2020-361

119.     Seybold, H., Andrade, J. S., & Herrmann, H. J. (2007). Modeling river delta formation. *Proceedings of the National Academy of Sciences*, *104*(43), 16804–16809. https://doi.org/10.1073/pnas.0705265104

120.     Sit, M., Demiray, B. Z., Xiang, Z., Ewing, G. J., Sermet, Y., & Demir, I. (2020). A comprehensive review of deep learning applications in hydrology and water resources. Water Science and Technology, 82(12), 2635–2670. https://doi.org/10.2166/wst.2020.369

121.     Simon & Collison. 2002. Quantifying the mechanical and hydrologic effects of riparian vegetation on streambank stability. Earth Surface Processes and Landforms 27(5): 527-546.

122.     Spreitzer, G., Tunnicliffe, J., & Friedrich, H. (2021). Effects of large wood (LW) blockage on Bedload Connectivity in the presence of a hydraulic structure. *Ecological Engineering*, *161*, 106156. https://doi.org/10.1016/j.ecoleng.2021.106156

123.     Sun, A. Y., & Scanlon, B. R. (2019). How can Big Data and machine learning benefit environment and water management: a survey of methods, applications, and future directions. Environmental Research Letters, 14(7), 073001. https://doi.org/10.1088/1748-9326/ab1b7d

124.     Tadaki, M., Brierley, G., & Cullum, C. (2014). River classification: theory, practice, politics. *WIREs Water*, *1*(4), 349–367. https://doi.org/10.1002/wat2.1026

125.     Tavares da Costa, R., Manfreda, S., Luzzi, V., Samela, C., Mazzoli, P., Castellarin, A., & Bagli, S. (2019). A web application for hydrogeomorphic flood hazard mapping. *Environmental Modelling & Software*, *118*, 172–186. https://doi.org/10.1016/j.envsoft.2019.04.010

126.     Tien Bui, D., Ho, T.-C., Pradhan, B., Pham, B.-T., Nhu, V.-H., & Revhaug, I. (2016). GIS-based modeling of rainfall-induced landslides using data mining-based functional trees classifier with AdaBoost, Bagging, and MultiBoost ensemble frameworks. Environmental Earth Sciences, 75(14), 1101. https://doi.org/10.1007/s12665-016-5919-4

127.     Varouchakis, E. A., Giannakis, G. V., Lilli, M. A., Ioannidou, E., Nikolaidis, N. P., & Karatzas, G. P. (2016). Development of a statistical tool for the estimation of riverbank erosion probability. SOIL, 2(1), 1–11. https://doi.org/10.5194/soil-2-1-2016

128.     Vasu, N. N., & Lee, S.-R. (2016). A hybrid feature selection algorithm integrating an extreme learning machine for landslide susceptibility modeling of Mt. Woomyeon, South Korea. Geomorphology, 263, 50–70. https://doi.org/10.1016/j.geomorph.2016.03.023

129.     Verstappen, H. T. (2011). Old and New Trends in Geomorphological and Landform Mapping. In Developments in Earth Surface Processes (Vol. 15, pp. 13–38). Elsevier. https://doi.org/10.1016/B978-0-444-53446-0.00002-1

130.     Wang, Z., Lai, C., Chen, X., Yang, B., Zhao, S., & Bai, X. (2015). Flood hazard risk assessment model based on random forest. Journal of Hydrology, 527, 1130–1141. https://doi.org/10.1016/j.jhydrol.2015.06.008

131.    Wang, W., Zhou, K., Jing, H., Zuo, J., Li, P., & Li, Z. (2019). Effects of Bridge Piers on Flood Hazards: A Case Study on the Jialing River in China. *Water*, *11*(6), 1181. https://doi.org/10.3390/w11061181

132.    Wheaton, J. M., Fryirs, K. A., Brierley, G., Bangen, S. G., Bouwes, N., & O'Brien, G. (2015). Geomorphic mapping and taxonomy of Fluvial landforms. *Geomorphology*, *248*, 273–295. https://doi.org/10.1016/j.geomorph.2015.07.010

133.    Wheeler, N., Pingram, M., David, B., Marson, W., Tunnicliffe, J., & Brierley, G. (2022). River adjustments, geomorphic sensitivity and management implications in the Waipā catchment, Aotearoa New Zealand. *Geomorphology*, 108263. https://doi.org/10.1016/j.geomorph.2022.108263

134.    Williams, R. D., Bangen, S., Gillies, E., Kramer, N., Moir, H., & Wheaton, J. (2020). Let the river erode! Enabling lateral migration increases geomorphic unit diversity. *Science of The Total Environment*, *715*, 136817. https://doi.org/10.1016/j.scitotenv.2020.136817

135.    Wu, Y., Ouyang, W., Hao, Z., Lin, C., Liu, H., & Wang, Y. (2018). Assessment of soil erosion characteristics in response to temperature and precipitation in a freeze-thaw watershed. *Geoderma*, *328*, 56–65. https://doi.org/10.1016/j.geoderma.2018.05.007

136.    Wing, O. E. J., Bates, P. D., Sampson, C. C., Smith, A. M., Johnson, K. A., & Erikson, T. A. (2017). Validation of a 30 m resolution flood hazard model of the conterminous United States. Water Resources Research, 53, 7968–1986

137.    Winterbottom, S.J., Gilvear, D.J. (2000) A GIS-based approach to mapping probabilities of river bank erosion: regulated River Tummel, Scotland. Regulated Rivers: Research & Management, 16, 127-140.

138.    Yochum, S. E., Sholtes, J. S., Scott, J. A., & Bledsoe, B. P. (2017). Stream power framework for predicting geomorphic change: The 2013 Colorado Front Range flood. *Geomorphology*, *292*, 178–192. https://doi.org/10.1016/j.geomorph.2017.03.004

# Appendix A: Test on non-trained watershed (Coaticook)

To test the model on an untrained watershed, we used the Coaticook River, where the Concordia and UQAR research teams had already carried out a freedom space (FS) analysis, enabling us to validate the results in relation to the river's floodplain and mobility space. However, the FS results do not allow us to determine the areas where incision is likely to occur and, consequently, the ML model developed for determining the type of erosion could not be validated. It is important to bear in mind the differences between the two approaches when interpreting the results of this analysis. The FS analysis maps areas that are likely to be flooded or eroded within the next 50 years (M50), whereas our model predicts where these fluvial hazards could occur along the river. Consequently, when classifying points using the FS results, the outcomes are large homogeneous groups of flood prediction, whereas our model creates more heterogeneous groups at the CRHQ reference points. For example, in our model, more sinuous areas have a greater chance of initiating a flooding event and are therefore classified as having a high probability of flooding, while more linear portions that may be affected by this flooding event but are less likely to contribute directly to flooding are predicted as having a low probability of flooding, or no flooding at all. As far as mobility results are concerned, the FS results map the area likely to erode over the next 50 years, meaning that areas where incision is occurring do not appear as mobile as they will not generate significant lateral migration. Similar problems arise in densely populated areas where anthropogenic structures reduce the capacity for lateral migration, making the area appear stable. As our model is trained to detect both incision and areas where erosion may occur, including in areas with anthropogenic structures, it will produce different results from those of the FS, as it will be able to predict that these areas are mobile, whereas according to the M50, they appear stable. Accuracy results should therefore be treated with caution, especially the presence of mobility results.

## A.1) Description of study area

The study area is located in the Appalachian Mountains and comprises the Canadian section of the Coaticook River (Figure A.1). This is a partially confined river with several large unconfined floodplains having highly meandering reaches that are prone to lateral migration and flooding, interrupted by geologically confined linear segments where the flood hazard is lower, and which
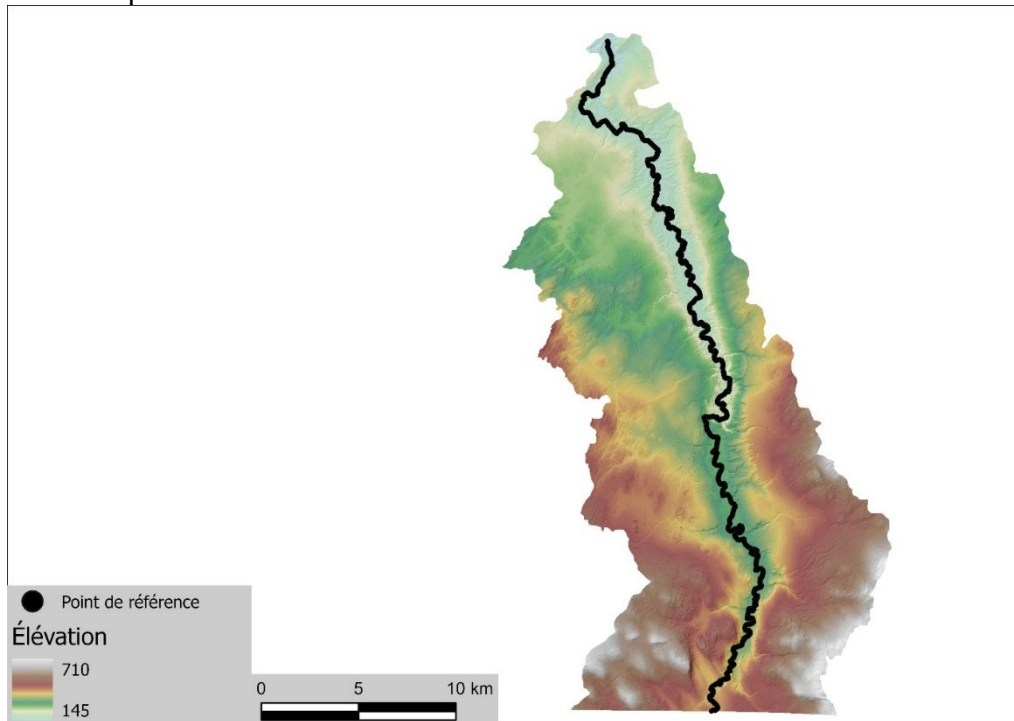
are more prone to incision.



*Figure A.1: Coaticook River study areas with CRHQ reference points overlaid over a 1-m DEM.*

## A.2) Prediction results for the Coaticook River

Figure A.2 and A.3 display the accuracy of the model as well as the percentage of points that had a confidence level greater than 55%. Figure A.2 shows that the accuracy of the flooding results was good, with accuracy levels ranging from 73% to 86%, despite the fact that the model was not trained on this catchment and the differences between the FS model used for validation and our model. Uncertainty was relatively low, ranging from 12% to 23%. Visually examining the results, the unconfined flood plains were predicted as high risk of flooding while the geologically confined portions being predicted as absence of flooding (Figure A.4). The PFM therefore produces very good results on watersheds it was not trained on. The mobility validation results (Figure A.3) were less good, with accuracy ranging from 53% to 67%. As mentioned above, it is important to interpret these results with caution due to differences in the way the validation data (FS model) and predicted data (our model) are generated for mobility. On visual examination of the results, the majority of wrongly predicted points were in geologically or anthropogenically confined areas that the FS model displayed as stable (minimal lateral migration) whereas our model predicted them as potentially problematic for infrastructure or sites with a potential for incision to occur. The number of points with confidence levels above 55% varied more for the mobility model, with a minimum value of 8% and a maximum of 29%. In Figure A.4 we can see that the PMM did not predict any part of this watershed as stable, but rather mobile with a high confidence of lateral migration in the floodplains and mobile with a medium confidence of incision in the confined areas. However, the Coaticook is a mobile river and examining the predictions in Figure A.4 we see that the majority of the river is predicted as low confidence levels of mobility with the most mobile areas being predicted with high confidence. This could be a result of the upstream conditions being indicative of a mobile river boosting the confidence

that the points are mobile and when combined with the correct values for local variables the mobility prediction becomes high confidence that this particular area will be impacted. Tests on other untrained watersheds that lacked validation data did produce stable predictions and therefore more tests are needed to verify if the fact that all the points were predicted as mobile was due to model error or were appropriate for this river. Overall, the PMM produced a useful map of the most mobile areas within the watershed while warning users that mobility could occur at most points in this watershed during large floods or if anthropogenic changes were made to the watershed that would increase the probability of mobility.
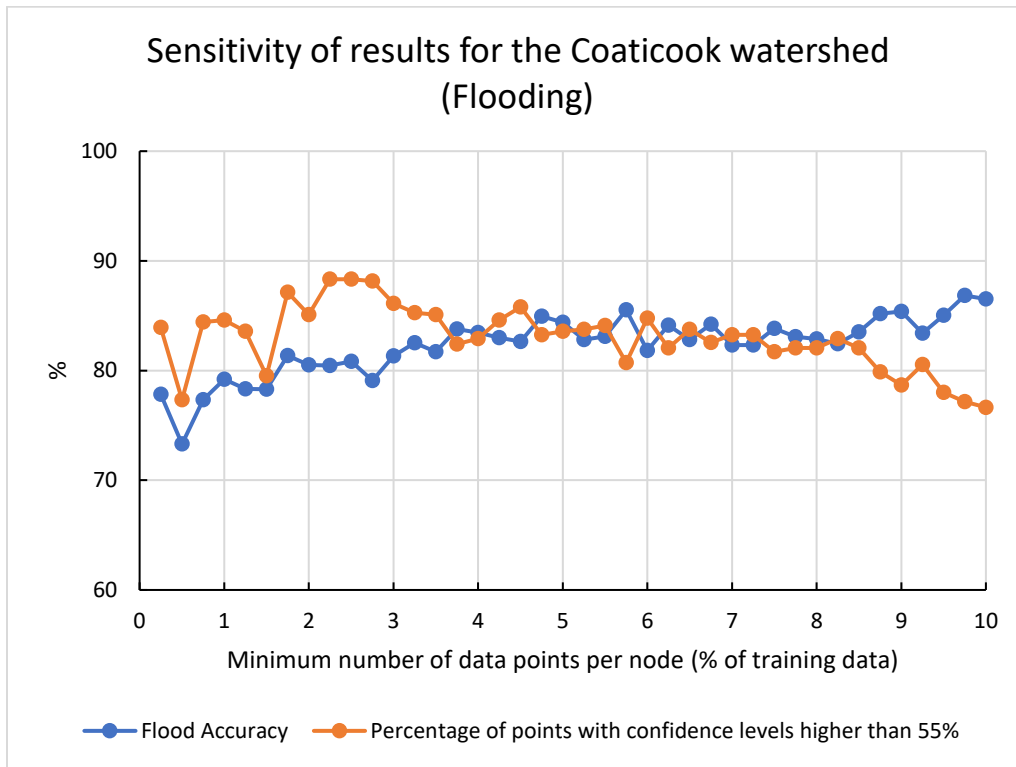


*Figure A.2: Sensitivity of results for the Coaticook watershed to the minimum number of data points per node for the presence of flooding, showing both accuracy and the percentage of points above the 55% confidence level.*
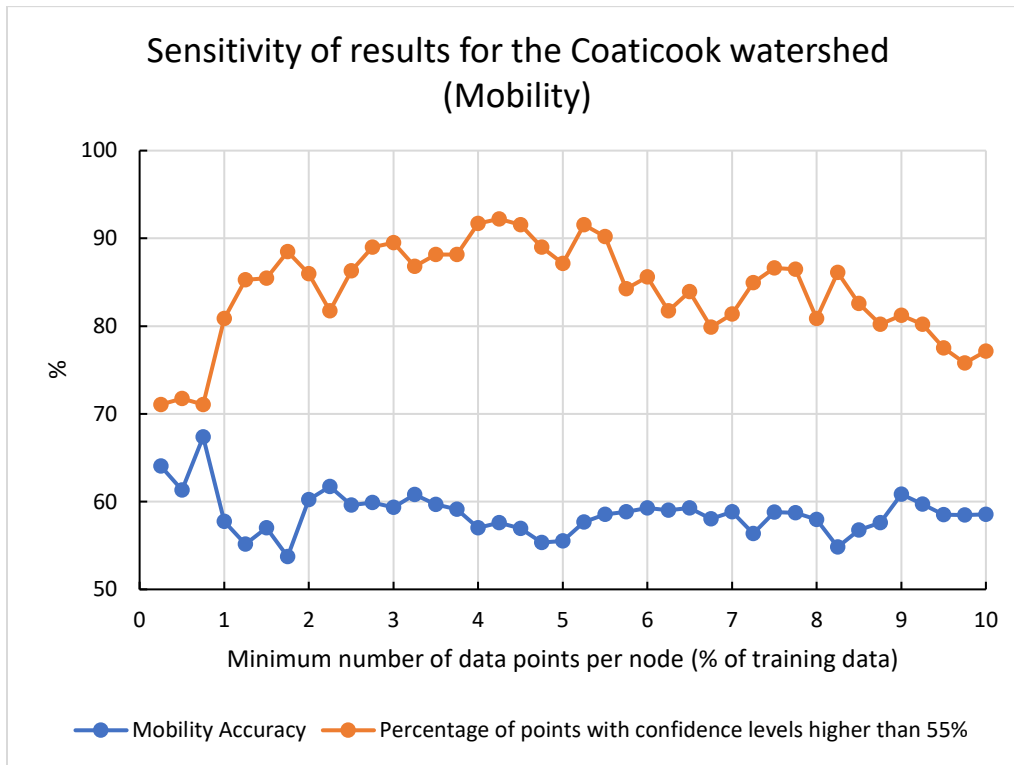
*Figure A.3: Sensitivity of results for the Coaticook watershed to the minimum number for the presence of mobility showing both accuracy and percentage of points above the 55% confidence level.*
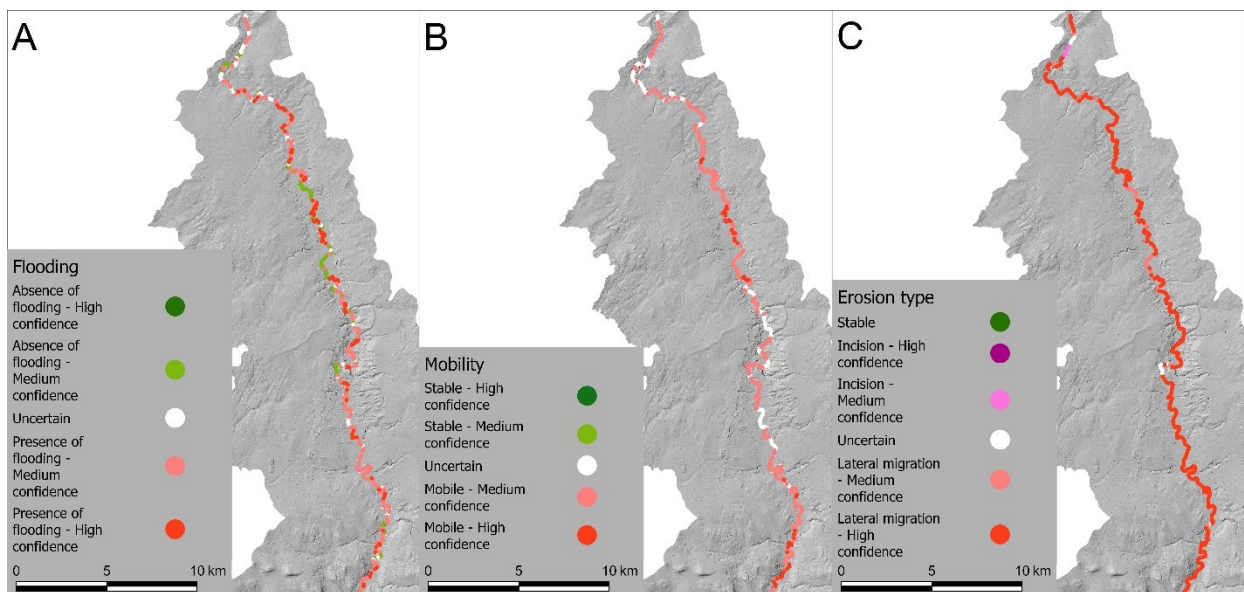


*Figure A.4: Results for the three models for an untrained watershed (Coaticook River, Quebec). A) results from the presence of flooding model, B) results from the presence of mobility model, and C) results from the type of erosion model*